Supersolid phase of three-dimensional spin- and hardcore-boson models

Hiroaki T. Ueda and Keisuke Totsuka
Yukawa Institute for Theoretical Physics, Kyoto University, Kitashirakawa Oiwake-Cho, Kyoto 606-8502, Japan
(Received 4 December 2009; published 25 February 2010)

We study the stability of solid- and supersolid (SS) phases of three-dimensional spin- and hardcore-Bose-Hubbard models on a body-centered cubic lattice. To see the quantum effects on the stability of the SS phase, we model the vacancies (interstitials) introduced in the solid, which are believed responsible for the appearance of the SS phase, by spin-wave bosons and adopt the interaction between the condensed bosons as a criterion. A repulsive nature of the low-energy effective interaction is the necessary condition for a second-order solid-SS transition and when this condition is met, normally the SS phase is expected. In calculating the effective interaction, we use expansions from the semiclassical (i.e., large S) and the Ising limit combined with the ladder approximation. The impact of quantum fluctuations crucially depends on the energy of the solid phase and that of the superfluid phase at half filling. As an application to ^{4}He, we study the parameter region in the vicinity of the fitting parameter set given by Liu and Fisher. For this parameters set, quantum fluctuations at the second order in S^{-1} destabilize the solid phase, which is supposed to be stable within the mean-field theory.

DOI: 10.1103/PhysRevB.81.054442 PACS number(s): 67.80.kb, 75.10.Jm, 67.80.bd, 75.45.+j

I. INTRODUCTION

The supersolid (SS) state, which has both diagonal- and off-diagonal long-range order, has been investigated over the past five decades.[1–3] Recently, Kim and Chan suggested[4] that the observed nonclassical rotational inertia (NCRI) (Ref. 5) in solid ^{4}He, might be attributed to coexisting superfluidity. This experiment sparked a renewed interest and the origin of the NCRI is still under debate.[6]

The quantum lattice gas (QGM) model,[7] or equivalently the hardcore-Bose-Hubbard model, is one of the simplest models suited for studying the low-temperature physics of quantum solids. Since the QGM is in an exact correspondence to $S=1/2$ quantum spin models,[7] we can use powerful methods developed in quantum spin systems in understanding the physics underlying the QGM. The QGM has been applied[8] to study the possibility of the SS in ^{4}He and later the comprehensive discussion[9] given by Liu and Fisher concluded, within the mean-field approximation (MFT) that the SS exists in ^{4}He. However, recent studies on the SS in the two-dimensional (2D) square lattice systems revealed that quantum fluctuations dramatically change the behavior and may even suppress the SS which is supposed to exist within the MFT.[10–12] For the optimal fitting parameter set obtained by Liu and Fisher for ^{4}He [*LF point*; see Eq. (3)], frustration seems to play an important role. Hence, interplay between quantum fluctuations and frustration may change the physics of the QGM of ^{4}He.

Recently, Bose-Einstein condensation (BEC) of magnons has been observed experimentally[13,14] and is now widely investigated.[15] Effects of frustration on magnon BEC would be intriguing in their own right, as frustration may enhance quantum effects and even lead to such exotic condensed states as the SS which are hardly realized in real Bose systems. For instance, quite recently, Takigawa *et al.* reported[16] a persisting spin superlattice in $SrCu_2(BO_3)_2$ (SCBO) (Ref. 17) coexisting with (possibly) mobile magnons even beyond the 1/8 plateau, which is reminiscent of the SS state predicted theoretically[18] for SCBO. Because weak anisotropic interactions break the rotational symmetry around the externally applied magnetic field [or, U(1) gauge symmetry in the QGM language], this phase may not a true SS phase. However, the discrete subgroup of the rotational symmetry can be spontaneously broken[19] and the observed phase might still hold a close relationship to the SS in its original sense. The physics of this phase and the realization of the "magnon SS" in other compounds are also topics to be investigated more closely.

For the clear understanding of NCRI in ^{4}He and the SS states in spin systems, it is useful to find a criterion which assesses the combined effect of quantum fluctuations and frustration on the stability of the SS phase. In this paper, with the help of spin-wave expansion, we push ahead with the widely accepted intuitive picture[2,3] that BEC of vacancies or interstitials gives rise to the SS state to propose that the interaction among the condensed vacancies (interstitials) serves as a good criterion for the stability of the SS. To this end, we adopt the so-called dilute-Bose-gas technique.[20] Normally, the dilute-Bose-gas approach is used *only* in the vicinity of the saturation field to obtain unbiased (asymptotically) exact results,[21–25] since the lack of an exact reference state (i.e., vacuum) on which boson excitations are defined hampers the construction of a well-defined bosonic Hamiltonian. To overcome this difficulty, we introduce the spin magnitude S and the Ising-like anisotropy as large control parameters, which guarantee the validity of the reference state even far below the saturation field and develop a systematic expansion with respect to these parameters.

The organization of the present paper is as follows. In Sec. II, we introduce a three-dimensional model Hamiltonian on a body-centered cubic (bcc) lattice (see Fig. 1) and briefly review the correspondence between the spin model and the QGM. At the same time, we classify the ground-state phases within the MFT. Then, we derive a spin-wave Hamiltonian by using the Dyson-Maleev transformation in the solid phase.

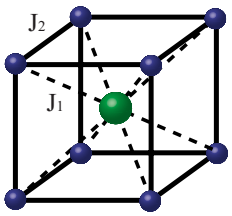

FIG. 1. (Color online) Three-dimensional bcc lattice and interactions considered in the text. Filled circles denote spins connected by anisotropic (*XXZ* like) exchange interactions. We divide the lattice into two sublattices, which are distinguished by the size of spheres. Each sublattice forms a simple cubic lattice.

In Sec. III, we outline the dilute-Bose-gas approach used in investigating the SS phase around the solid phase. If the effective interaction among the condensed bosons is attractive, the SS phase for low condensate density is normally phase separated. Although we do not exclude the possibility that the SS emerges through the first-order transition from the solid phase, this seems unlikely from various results obtained by quantum Monte Carlo simulations.[10–12,26–28] Hence, in this paper, the SS is said to be "unstable" ("stable") if the interaction between condensed bosons is attractive (repulsive). To evaluate the interaction concretely, we need approximations. In Sec. IV, we study the properties of the solid and the SS phase by the large S expansion up to the second order in S^{-1}. At the first order, the MFT results are reproduced. We shall find three types of SSs, which have properties similar to those appearing in the 2D square lattice.[27,29–31] The formulation of the second-order perturbation is detailed.

In Sec. V, we study the properties of the solid and the SS phase by the Ising expansion up to the second order. Although quantum fluctuations seem to suppress the interactions at the first order, the boundary determining the stability of the SS does not shift and the magnetization process is affected only quantitatively by quantum fluctuations. In other words, the stability itself is known from the MFT if the large Ising anisotropy exists. To see the effect of quantum fluctuations on the stability of SS, we have to proceed to the second-order calculation.

Our main results are summarized in Sec. VI, where we study the stability of the solid and the SS phases focusing on the LF point. Readers who only want to know the main results may skip Secs. IV and V and go directly to this section. For the parameter set corresponding to the LF point, quantum fluctuations destabilize the solid state expected from the MFT (Fig. 11) at least within the conventional second-order spin-wave expansion. Concerning the stability of the SS, both of the two second-order calculations conclude that quantum fluctuations only slightly change the MFT boundary of the SS phase, provided that the energy of the solid phase is sufficiently smaller than that of the superfluid phase at half filling (Fig. 14). In the vicinity of the LF point, where the above condition is not satisfied, it is suggested that the SS phase is fragile against quantum corrections or even completely smeared out, although the validity of both approaches is not obvious in this region.

For concreteness, we restrict our discussion in this paper to a quantum spin model on a bcc lattice. However, our approach can be easily generalized to quantum spin models on other three-dimensional (3D) lattices.

II. SPIN HAMILTONIAN AND QUANTUM LATTICE GAS MODEL

A. Model Hamiltonian

Let us consider the following frustrated spin Hamiltonian on the bcc lattice with the nearest-neighbor Ising antiferromagnetic (AF) interactions ($J_1^z>0$)

$$H=\sum_{\text{n.n.}}\{J_1^z S_{\mathbf{i}}^z S_{\mathbf{j}}^z+J_1^{\perp}(S_{\mathbf{i}}^x S_{\mathbf{j}}^x+S_{\mathbf{i}}^y S_{\mathbf{j}}^y)\}+\sum_{\text{n.n.n.}}\{J_2^z S_{\mathbf{i}'}^z S_{\mathbf{j}'}^z+J_2^{\perp}(S_{\mathbf{i}'}^x S_{\mathbf{j}'}^x+S_{\mathbf{i}'}^y S_{\mathbf{j}'}^y)\}+Sh\sum_{\mathbf{i}} S_{\mathbf{i}}^z, \quad (1)$$

where the summations nearest neighbors and next-nearest neighbors are taken for the nearest-neighbor and the second-nearest-neighbor pairs, respectively. This Hamiltonian in the case that $J_i^z=J_i^{\perp}$ for $i=\{1,2\}$ (Heisenberg case) has been investigated from the various approaches.[32] In the case of $S=1/2$, this Hamiltonian is equivalent to the following hard-core bosonic Hubbard model,[33]

$$H=\sum_{\text{n.n.}}\left\{\frac{J_1^{\perp}}{2}(p_{\mathbf{i}}^{\dagger}p_{\mathbf{j}}+p_{\mathbf{i}}p_{\mathbf{j}}^{\dagger})+J_1^z\hat{n}_{\mathbf{i}}\hat{n}_{\mathbf{j}}\right\}+\sum_{\text{n.n.n.}}\left\{\frac{J_2^{\perp}}{2}(p_{\mathbf{i}'}^{\dagger}p_{\mathbf{j}'}+p_{\mathbf{i}'}p_{\mathbf{j}'}^{\dagger})+J_2^z\hat{n}_{\mathbf{i}'}\hat{n}_{\mathbf{j}'}\right\}-\mu_h\sum_{\mathbf{i}}\hat{n}_{\mathbf{i}}, \quad (2)$$

where $\hat{n}_{\mathbf{i}}=p_{\mathbf{i}}^{\dagger}p_{\mathbf{i}}$. This model can be used to study the low-energy physics of ^{4}He if we approximate the Bose gas by the QGM.[7] Specifically, the "longitudinal" couplings $J_{1,2}^z$ and "transverse" ones $J_{1,2}^{\perp}$ mimic the interaction potentials and the kinetic energy of Helium, respectively, and the external magnetic field h (or μ_h) controls the pressure. In the QGM, $J_{1,2}^{\perp}<0$ and $J_1^{\perp}/J_2^{\perp}$ is fixed at 1/2 because of the lattice structure. Liu and Fisher suggested several sets of fitting parameters appropriate for ^{4}He and concluded that the stability of the SS phase is ensured within the MFT.[9] However, the existence of quantum fluctuations and frustration effects may destroy the classical ground state. To see the validity of the MFT, in Sec. VI we shall study these effects on the ground state in the vicinity of the following parameter set [LF point; the case (a) in Ref. 9]:

$$J_1^z=2.60, \quad J_2^z=1.59, \quad J_1^{\perp}=-1, \quad J_2^{\perp}=-0.5. \quad (3)$$

Since the Ising-like Néel antiferromagnetic (NAF) phase is identified with a solid phase of ^{4}He, we restrict ourselves only to the case that NAF order along the z direction appears around $h=0$ and will not consider the Ising-like collinear antiferromagnetic (CAF) phase which realizes, in the classical case, when $2J_1^z<3J_2^z$. Let us briefly discuss possible classical phases at $h=0$. The classical phases fall into three fundamental classes (NAF, CAF, and FM) as is shown in Fig. 2. These phases are further classified by whether the spins align along the z axis or in the xy plane. In the former case, the ground state may be gapped. In the latter case, the spontane-

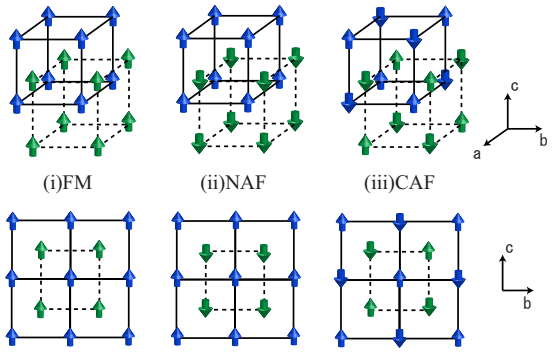

FIG. 2. (Color online) Spin configurations for the three phases (FM, NAF, and CAF') in the text. (i) FM (ferromagnetic phase) represents a phase where all spins are polarized along the field direction. (ii) In NAF, the spins on each sublattice align ferromagnetically while those on different sublattices are antiparallel. (iii) CAF is made up of two antiferromagnetically ordered sublattices, which, as a whole, align in a collinear manner.

ous symmetry breaking of the rotational symmetry around the z-axis $[U(1)]$ induces the gapless Goldstone mode and the phase is viewed as a superfluid (SF). The $U(1)$ broken phases accompanied by translation-symmetry breaking in the *diagonal* channel (i.e., $\langle p_{\mathbf{l}}^{\dagger} p_{\mathbf{l}} \rangle$ or $\langle S_{\mathbf{l}}^{z} \rangle$) as well are thought of as spin analogs of SSs.[29,30]

When the spins align in z axis, the energy of each Ising-like phase is given by

$$\frac{E_{\text{Ising-NAF}}}{2NS^2} = -4J_1^z + 3J_2^z, \tag{4a}$$

$$\frac{E_{\text{Ising-CAF}}}{2NS^2} = -3J_2^z, \tag{4b}$$

$$\frac{E_{\text{Ising-FM}}}{2NS^2} = 4J_1^z + 3J_2^z - |h|, \tag{4c}$$

where N is the number of sites of each sublattice. When the spins align in xy plane, the phases are viewed as SFs and the energy of each phase is given by

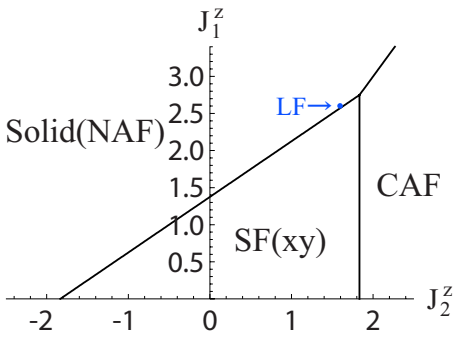

FIG. 3. (Color online) Classical phase diagram for $h=0$, $J_1^{\perp}=-1$, and $J_2^{\perp}=-1/2$. NAF and CAF are implied as the Ising-like gaped ones. The dot labeled as LF represents the LF point (3).

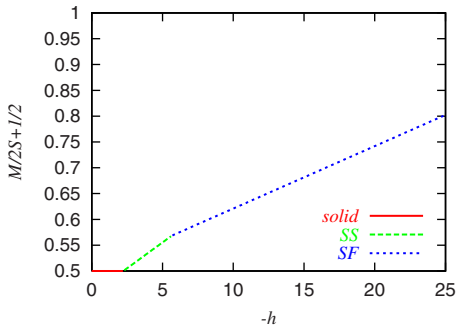

FIG. 4. (Color online) The magnetization curve obtained for the LF point (3) within the MFT. Magnetization M is given by $(1/2N)\Sigma_1^{2N}\langle S_{\mathbf{i}}^{z} \rangle$. The existence of the phase solid, SS and SF is confirmed.

$$\frac{E_{\text{xy-NAF}}}{2NS^2} = -4J_1^{\perp} + 3J_2^{\perp}, \tag{5a}$$

$$\frac{E_{\text{xy-CAF}}}{2NS^2} = -3J_2^{\perp}, \tag{5b}$$

$$\frac{E_{\text{xy-FM}}}{2NS^2} = 4J_1^{\perp} + 3J_2^{\perp}. \tag{5c}$$

The ground-state phase diagram of the QGM for $h=0$ and $J_1^{\perp}/J_2^{\perp}=1/2$ is shown in Fig. 3.

The magnetization curve for the LF point (3) is shown in Fig. 4.

To see the physics of the NAF phase more clearly, we divide the whole lattice into two sublattices A and B each of which forms a cubic lattice. Since we can change the sign of the (nearest neighbor) transverse coupling $J_1^{\perp} \to -J_1^{\perp}$ at will by making spin rotation (by π) around the z axis $S_l^i \to -S_l^i (i = x, y, l \in A)$ only for the A sublattice, we may restrict our consideration to the case $J_1^{\perp} \leq 0$.

The correspondence between the phases in the quantum lattice-gas formulation and the ones in the (quantum) spin-model formulation is shown in Table I. In Table I, the long-distance limit $|\mathbf{i}-\mathbf{j}| \to \infty$ is implied. In the SS phase and its spin counterpart, translation symmetry is spontaneously broken (i.e., $\langle S_{\mathbf{i}}^{z} \rangle$ and $\langle n_{\mathbf{i}} \rangle$ modulate in space with nontrivial periods) as well as the axial $U(1)$.

In this paper, we reserve the terminology "NAF" for the Ising-like NAF phase and the corresponding phase in the

TABLE I. Correspondence between the QGM and the spin model. "TS" denotes translational symmetry.

QGM (Bose-Hubbard model)	Spin model
Vacuum	(polarized) FM
Checkerboard solid	(Ising-like) NAF
Striped solid	(Ising-like) CAF
SF ($\langle p_{\mathbf{i}} p_{\mathbf{j}} \rangle \neq 0$ with TS)	$\langle S_{\mathbf{i}}^{+} S_{\mathbf{j}}^{+} \rangle \neq 0$ with TS
SS ($\langle p_{\mathbf{i}} p_{\mathbf{j}} \rangle \neq 0$ with broken TS)	$\langle S_{\mathbf{i}}^{+} S_{\mathbf{j}}^{+} \rangle \neq 0$ with broken TS

Bose-Hubbard model (2) will be called (checkerboard) "solid" or "half-filled solid."

B. Spin-wave Hamiltonian

In order to rewrite the spin operators in terms of bosons, it is convenient to define magnons over a presumed reference state. In the case of NAF, all spins on the A-sublattice point upward and those on the B-sublattice downward (see Fig. 2). Therefore, it would be reasonable to introduce the following antiferromagnetic Dyson-Maleev (ADM) transformation,[34–36]

$$S_{\mathbf{l}}^{+} = \sqrt{2S}a_{\mathbf{l}}, \quad S_{\mathbf{l}}^{-} = \sqrt{2S}a_{\mathbf{l}}^{\dagger}\left(1 - \frac{a_{\mathbf{l}}^{\dagger}a_{\mathbf{l}}}{2S}\right),$$

$$S_{\mathbf{l}}^{z} = S - a_{\mathbf{l}}^{\dagger}a_{\mathbf{l}}, \quad \text{for } \mathbf{l} \in \mathrm{A}. \tag{6a}$$

$$S_{\mathbf{m}}^{+} = \sqrt{2S}b_{\mathbf{m}}^{\dagger}, \quad S_{\mathbf{m}}^{-} = \sqrt{2S}\left(1 - \frac{b_{\mathbf{m}}^{\dagger}b_{\mathbf{m}}}{2S}\right)b_{\mathbf{m}},$$

$$S_{\mathbf{m}}^{z} = -S + b_{\mathbf{m}}^{\dagger}b_{\mathbf{m}}, \quad \text{for } \mathbf{m} \in \mathrm{B}. \tag{6b}$$

If we introduce the Fourier transformation as

$$a_{\mathbf{l}} = \frac{1}{\sqrt{N}}\sum_{\mathbf{k}} a_{\mathbf{k}}e^{i\mathbf{k}\cdot\mathbf{l}}, \quad b_{\mathbf{m}} = \frac{1}{\sqrt{N}}\sum_{\mathbf{k}} b_{\mathbf{k}}e^{i\mathbf{k}\cdot\mathbf{m}}, \tag{7}$$

(N is the number of sites of each sublattice), then the Hamiltonian is given by

$$H = H_0 + H_1 + \text{const}, \tag{8a}$$

$$H_0 = \sum_{\mathbf{k}} S\{[\epsilon_0(\mathbf{k}) - h]a_{\mathbf{k}}^{\dagger}a_{\mathbf{k}} + [\epsilon_0(\mathbf{k}) + h]b_{\mathbf{k}}^{\dagger}b_{\mathbf{k}} + t_0(\mathbf{k})(a_{\mathbf{k}}b_{-\mathbf{k}} + a_{\mathbf{k}}^{\dagger}b_{-\mathbf{k}}^{\dagger})\}, \tag{8b}$$

$$H_1 = \frac{1}{N}\sum_{\mathbf{k}_1,\mathbf{k}_2,\mathbf{q}} \{-2J_1^z C_1(\mathbf{q})a_{\mathbf{k}_1+\mathbf{q}}^{\dagger}b_{\mathbf{k}_2-\mathbf{q}}^{\dagger}a_{\mathbf{k}_1}b_{\mathbf{k}_2} + [J_2^z C_2(\mathbf{q}) - J_2^{\perp}C_2(\mathbf{k}_2)]a_{\mathbf{k}_1+\mathbf{q}}^{\dagger}a_{\mathbf{k}_2-\mathbf{q}}^{\dagger}a_{\mathbf{k}_1}a_{\mathbf{k}_2} + [J_2^z C_2(\mathbf{q}) - J_2^{\perp}C_2(\mathbf{k}_2 - \mathbf{q})]b_{\mathbf{k}_1+\mathbf{q}}^{\dagger}b_{\mathbf{k}_2-\mathbf{q}}^{\dagger}b_{\mathbf{k}_1}b_{\mathbf{k}_2} - J_1^{\perp}C_1(\mathbf{k}_2)(a_{\mathbf{k}_1+\mathbf{q}}^{\dagger}a_{\mathbf{k}_2-\mathbf{q}}^{\dagger}a_{\mathbf{k}_1}b_{-\mathbf{k}_2}^{\dagger} + b_{\mathbf{k}_1+\mathbf{q}}^{\dagger}b_{\mathbf{k}_2+\mathbf{q}}b_{\mathbf{k}_1}a_{-\mathbf{k}_2})\}, \tag{8c}$$

where

$$\epsilon_0(\mathbf{k}) = 8J_1^z - 6J_2^z + 2J_2^{\perp}C_2(\mathbf{k}), \tag{9a}$$

$$t_0(\mathbf{k}) = 2J_1^{\perp}C_1(\mathbf{k}), \tag{9b}$$

$$C_1(\mathbf{k}) = 4\cos\frac{k_x}{2}\cos\frac{k_y}{2}\cos\frac{k_z}{2}, \tag{9c}$$

$$C_2(\mathbf{k}) = \cos k_x + \cos k_y + \cos k_z. \tag{9d}$$

Although this Hamiltonian is not hermitian and contains unphysical states,[34] we believe that the Hamiltonian given by Eqs. (8a)–(8c) correctly captures the low-energy physics at and around the half-filled solid. Actually, in the case of magnon BEC just below the saturation field, though generally not proven, it is known for some specific models that the ferromagnetic Dyson-Maleev transformation, the Holstein-Primakoff transformation and the hardcore-boson expansion for the $S=1/2$ case give the same ground state in a dilute-Bose-gas approach.[21–24]

III. GENERAL FORMALISM

In this section, we outline the dilute-Bose-gas approach by which we shall investigate the SS phase around the half-filled solid appearing in the system described by the Hamiltonian Eq. (8).

A. Bogoliubov transformation

In the following analysis, we frequently deal with Hamiltonians of the following form:

$$H_{\text{quad}} = S\{[\epsilon(\mathbf{k}) - h]a_{\mathbf{k}}^{\dagger}a_{\mathbf{k}} + [\epsilon(\mathbf{k}) + h]b_{\mathbf{k}}^{\dagger}b_{\mathbf{k}} + t(\mathbf{k})(a_{\mathbf{k}}b_{-\mathbf{k}} + a_{\mathbf{k}}^{\dagger}b_{-\mathbf{k}}^{\dagger})\}. \tag{10}$$

This is the most general quadratic Hamiltonian allowed by hermiticity and sublattice symmetry. When we consider the quadratic part (8b) of the Hamiltonian H, the functions $\epsilon(\mathbf{k})$ and $t(\mathbf{k})$ should be taken as

$$\epsilon(\mathbf{k}) = \epsilon_0(\mathbf{k}), \quad t(\mathbf{k}) = t_0(\mathbf{k}), \tag{11}$$

However, since the interaction H_1 shifts the grounds state, the renormalized quadratic Hamiltonian which leads to the exact Green's function including the self-energy do not in general coincide with Eq. (8b). Generically the functions $\epsilon(\mathbf{k})$ and $t(\mathbf{k})$ are given by

$$\epsilon(\mathbf{k}) = \epsilon_0(\mathbf{k}) + \epsilon'(\mathbf{k}), \quad t(\mathbf{k}) = t_0(\mathbf{k}) + t'(\mathbf{k}), \tag{12}$$

where $\epsilon'(\mathbf{k})$ and $t'(\mathbf{k})$ are of the order of S^{-1} since the interaction H_1 is of the order of S^0. In this paper, we approximately calculate the functions $\epsilon'(\mathbf{k})$ and $t'(\mathbf{k})$ in powers of S^{-1} (Sec. IV) or of the Ising coupling constant $1/J_1^z$ (Sec. V). Now let us assume that we have found an appropriate H_{quad}. Then, in order to eliminate the off-diagonal terms $ab+a^{\dagger}b^{\dagger}$, we may introduce the following Bogoliubov transformation:

$$a_{\mathbf{k}} = \cosh\theta_{\mathbf{k}}\alpha_{\mathbf{k}} - \sinh\theta_{\mathbf{k}}\beta_{\mathbf{k}}^{\dagger}, \tag{13a}$$

$$b_{\mathbf{k}} = -\sinh\theta_{\mathbf{k}}\alpha_{\mathbf{k}}^{\dagger} + \cosh\theta_{\mathbf{k}}\beta_{\mathbf{k}}, \tag{13b}$$

which transforms H_{quad} to

$$H_{\text{quad}} = S\{(\epsilon_{\alpha}(\mathbf{k}) - h)\alpha_{\mathbf{k}}^{\dagger}\alpha_{\mathbf{k}} + [\epsilon_{\beta}(\mathbf{k}) + h]\beta_{\mathbf{k}}^{\dagger}\beta_{\mathbf{k}} + f(\mathbf{k},\theta_{\mathbf{k}}) \times(\alpha_{\mathbf{k}}\beta_{-\mathbf{k}} + \alpha_{\mathbf{k}}^{\dagger}\beta_{-\mathbf{k}}^{\dagger})\}. \tag{14}$$

In the above, we have introduced two functions

$$\epsilon_{\alpha}(\mathbf{k}) = \epsilon_{\beta}(\mathbf{k}) \equiv \epsilon(\mathbf{k})\cosh 2\theta_{\mathbf{k}} - t(\mathbf{k})\sinh 2\theta_{\mathbf{k}}, \tag{15a}$$

$$f(\mathbf{k},\theta_{\mathbf{k}}) \equiv -\epsilon(\mathbf{k})\sinh 2\theta_{\mathbf{k}} + t(\mathbf{k})\cosh 2\theta_{\mathbf{k}}. \tag{15b}$$

If we choose $\theta_{\mathbf{k}}$ in such a way that $f(\mathbf{k},\theta_{\mathbf{k}})=0$, i.e.,

$$\tanh 2\theta_{\mathbf{k}} = \frac{t(\mathbf{k})}{\epsilon(\mathbf{k})}, \tag{16}$$

H_{quad} is diagonalized and reads

$$H_{\text{quad}} = S[\epsilon_\alpha(\mathbf{k}) - h]\alpha_{\mathbf{k}}^\dagger \alpha_{\mathbf{k}} + S[\epsilon_\alpha(\mathbf{k}) + h]\beta_{\mathbf{k}}^\dagger \beta_{\mathbf{k}}, \tag{17}$$

It is important to note that the magnetic field h has different signs for α and β. Assuming the (unique) minimum of the spin-wave excitation $\epsilon_\alpha(\mathbf{k})$ takes place at $\mathbf{k}=\mathbf{Q}$, we may introduce the renormalized chemical potential by

$$\mu_\alpha \equiv h - \epsilon_\alpha(\mathbf{Q}). \tag{18}$$

Now suppose we increase the external magnetic field h (or μ_α). Then, the gap of the α (β) boson decreases (increase) and the α bosons into an α-SF phase discussed below.

B. Supersolid from magnon BEC

In the previous subsection, we have seen that, as the external magnetic field is increased, the α magnon condenses at $\mu_\alpha=0$ while the other remains gapped. Now, we show that this BEC of the Bogoliubov-transformed magnons generally leads to an SS phase. When a BEC occurs for $\mu_\alpha \geq 0$, $\alpha_{\mathbf{Q}}$ takes a finite expectation value $\langle \alpha_{\mathbf{Q}} \rangle \neq 0$ and, correspondingly, the original bosons a and b have the following expectation values:[39]

$$\langle a_{\mathbf{Q}} \rangle = \cosh\ \theta_{\mathbf{Q}} \langle \alpha_{\mathbf{Q}} \rangle, \quad \langle b_{\mathbf{Q}} \rangle = -\sinh\ \theta_{\mathbf{Q}} \langle \alpha_{\mathbf{Q}}^\dagger \rangle. \tag{19}$$

In a dilute-gas limit, when translated into the spin language, this implies the following spin configuration:[40]

$$\langle S_{\mathbf{l}}^x \rangle = \sqrt{2S\rho}\cosh\ \theta_{\mathbf{Q}} \cos(\mathbf{Q}\cdot\mathbf{l} + \varphi)\left(1 + \frac{f(\Delta S)}{S}\right),$$

$$\langle S_{\mathbf{l}}^y \rangle = \pm \sqrt{2S\rho}\cosh\ \theta_{\mathbf{Q}} \sin(\mathbf{Q}\cdot\mathbf{l} + \varphi)\left(1 + \frac{f(\Delta S)}{S}\right),$$

$$\langle S_{\mathbf{l}}^z \rangle = (S - \Delta S) - \rho \cosh^2\ \theta_{\mathbf{Q}}, \quad \text{for } \mathbf{l} \in \text{A}, \tag{20a}$$

$$\langle S_{\mathbf{m}}^x \rangle = -\sqrt{2S\rho}\sinh\ \theta_{\mathbf{Q}} \cos(\mathbf{Q}\cdot\mathbf{m} + \varphi)\left(1 + \frac{f(\Delta S)}{S}\right),$$

$$\langle S_{\mathbf{m}}^y \rangle = \mp \sqrt{2S\rho}\sinh\ \theta_{\mathbf{Q}} \sin(\mathbf{Q}\cdot\mathbf{m} + \varphi)\left(1 + \frac{f(\Delta S)}{S}\right),$$

$$\langle S_{\mathbf{m}}^z \rangle = -(S - \Delta S) + \rho \sinh^2\ \theta_{\mathbf{Q}}, \quad \text{for } \mathbf{m} \in \text{B}, \tag{20b}$$

where the real-space wave function is given by $\langle \alpha_{\mathbf{r}} \rangle = \sqrt{\rho}\ \exp\{\pm i(\mathbf{Q}\cdot\mathbf{r} + \varphi)\}$ and $\Delta S = 1/N\Sigma_q \sinh^2\ \theta_q$. The function $f(\Delta S) = \Delta S/2 + O(1/S)$ is obtained from the Holstein-Primakoff transformed operator $S^\pm$ and is independent of $\rho_{\mathbf{Q}}$ in the dilute-gas limit. One can easily see that this state may be thought of as an SS of magnons; an off-diagonal long-range (incommensurate) xy order (which translates into an SF long-range order) and a diagonal (commensurate) two-sublattice z order coexist with each other. In general, a modulation in the transverse component $S^{x,y}$ with the wave vector $\mathbf{Q}$ is incommensurate with the pattern of the z order.

If we denote the effective two-body interaction among the condensed bosons evaluated at $\mu_\alpha = 0^-$ by Γ, the leading term of the system energy is in general written, as a function of the condensate density ρ, as

$$\frac{E_{\text{eff}}}{N} \approx \text{const} + \frac{1}{2}\Gamma\rho^2 - S\mu_\alpha\rho. \tag{21}$$

Then, provided $\Gamma > 0$, ρ is given by minimizing E

$$\frac{\rho}{S} = \frac{\mu_\alpha}{\Gamma}, \quad \text{for } \mu_\alpha \geq 0. \tag{22}$$

However, the condition $\Gamma > 0$ is *not* sufficient condition for the stability of the SS phase since there may be higher-order terms with negative coefficients in E_{eff}, which may select a very large value of ρ and eventually destabilize the SS phase. If $\Gamma \leq 0$, on the other hand, one may expect a phase separation accompanied by magnetization jump near $\mu_\alpha = 0$. For both cases, there exists an additional possibility of more exotic phases where single-particle BECs are no longer relevant.[24]

The low-energy excitation spectrum of the SS phase is easily obtained as in the ordinary superfluid Bose gas.[37] Defining $\mathbf{k} \equiv \mathbf{q} - \mathbf{Q}$, we may expand $\epsilon_\alpha(\mathbf{q}) = \epsilon_{\min} + k_i k_j/(2m_{ij}) + \cdots$, where the summation over repeated indices is implied. We can diagonalize m_{ij} to obtain a standard dispersion $k_i k_j/2m_{ij} = k_i'^2/(2m_i') \equiv \epsilon_{\text{g}}(\mathbf{k}')$. Using this notation, the excitation spectrum of the SS phase is given by

$$\Omega_{\text{SS}}(\mathbf{k}) = \sqrt{\epsilon_{\text{g}}(\mathbf{k})^2 + 2S\mu_{\text{R}}\epsilon_{\text{g}}(\mathbf{k})} \approx \sqrt{2S\mu_{\text{R}}\epsilon_{\text{g}}(\mathbf{k})}. \tag{23}$$

For finite temperature, the Bose condensed bosons are suppressed, and the critical temperature is given by

$$k_{\text{B}}T_{\text{c}} = 2.087(m_x m_y m_z)^{-1/3}\left(\frac{S\mu_\alpha}{\Gamma}\right)^{2/3}. \tag{24}$$

For $T > T_{\text{c}}$, the long-range order disappears and $\langle S^\pm \rangle = 0$.

Above discussions assume the dilute-gas limit, where the scattering length is much smaller than the average interatomic distance $\rho^{-1/3}$. Specifically, our approximation is valid when

$$\Gamma(m_x m_y m_z \rho)^{1/3} \ll 1. \tag{25}$$

To summarize, the knowledge about the wave number $\mathbf{Q}$ at which the magnon BEC occurs, the effective mass m_i and the effective (two-body) interaction Γ for the condensed bosons enables us to derive the stability, the spin configuration which is not commensurate with the assumed sublattice structure, the quasiparticle excitation spectrum and the critical temperature of the SS phase. Therefore, the analysis boils down to the calculation of $\mathbf{Q}$ and Γ. A remark is in order here about the definition of the bosonic vacuum. In Eq. (6a) and (6b), it is implicitly assumed that the NAF phase gives a well-defined vacuum (i.e., the ground state when the condensate is absent) for the two bosons. In general, the NAF state shown in Fig. 2 suffers from quantum fluctuations and the above assumption is justified either for the semiclassical (i.e., large S) case or the Ising-like (i.e., large-$J_1^z/J_1^\perp$) limit[41]

In the following sections, we carry out the calculation by combining the ladder approximation with the large S and the Ising expansions. Concretely, in Sec. IV, we will obtain Eq. (12) and the interaction Γ by the large S expansion up to the second order in S^{-1}. At the first order, our approach will reproduce the results of the MFT; there are three types of SSs. At the second-order perturbation, quantum fluctuations may change the properties of the solid and the SSs qualitatively. However, we will see that the large-S expansion is not reliable to calculate Γ when the Ising-like anisotropy J_1^z is large. To overcome this difficulty, we will study Eq. (12) and Γ by the Ising expansion up to the second order in Sec. V. At the first order, quantum fluctuations suppress the interactions, but the stability of the SS itself is known by the MFT. Although we will find the stable bound-magnon state, this condensed phase may be phase separated for large J_1^z. In the second order, we will see the effect of quantum fluctuations on the stability of SS clearly.

IV. PERTURBATION THEORY IN S^{-1}

In this section, we study the physics of the SS phase by the perturbation theory in the parameter S^{-1}. The first-order calculation gives the same ground-state phases as the MFT. At the second order, on the other hand, quantum fluctuations play an important role and may destroy the classically stable solid (NAF) or the SS phase.

A. First-order perturbation

If we assume $\theta_{\mathbf{k}}$ by

$$\tanh 2\theta_{\mathbf{k}}^{(1)} = \frac{t_0(\mathbf{k})}{\epsilon_0(\mathbf{k})} = \frac{J_1^{\perp} C_1(\mathbf{k})}{4J_1^z - 3J_2^z + J_2^{\perp} C_2(\mathbf{k})}, \tag{26}$$

the quadratic part of the Hamiltonian is diagonalized up to $O(S)$ [see Eq. (12)]. We note that $\theta_k^{(1)}$ is well-defined when $|\tanh 2\theta_{\mathbf{k}}^{(1)}| \le 1$. Concretely, the half-filled solid is stable at $h=0$ when

$$4J_1^z - 3J_2^z + 3J_2^{\perp} \ge 4|J_1^{\perp}|. \tag{27}$$

If this inequality is not satisfied, the spins align in the xy plane (SF) [see Eqs. (4) and (5)]. Meanwhile, even when the classical ground state is CAF ($2J_1^z < 3J_2^z$), this inequality may be satisfied and then the metastable NAF phase against the one magnon fluctuation may be obtained. In this paper, we will not discuss the CAF case any more.

Let us discuss the minimum of the dispersion $\epsilon_{\alpha}(\mathbf{k}) = \epsilon_{\mathrm{S1}}^{(1)}(\mathbf{k})$ [see Eq. (15a)] to determine the structure of the SS. From Eq. (26), the dispersion relation reads,

$$\begin{aligned}\epsilon_{\mathrm{S1}}^{(1)}(\mathbf{k}) &= \sqrt{\epsilon_0(\mathbf{k})^2 - t_0(\mathbf{k})^2} \\ &= \sqrt{[8J_1^z - 6J_2^z + 2J_2^{\perp} C_2(\mathbf{k})]^2 - 4J_1^{\perp 2} C_1(\mathbf{k})^2}. \end{aligned} \tag{28}$$

where the superscript (i) of $\epsilon_{\mathrm{S1}}^{(i)}(\mathbf{k})$ denotes that the function is evaluated at $\theta_k = \theta_k^{(i)}$. In the following we shall use this notation to the other arbitral functions of $\theta_{\mathbf{k}}$. The minimum is obtained by setting $\mathbf{Q}=\mathbf{Q}_1=(0,0,0)$ or $\mathbf{Q}_2=(\pi,\pi,\pi)$. Although we cannot exclude other possibilities generally, this is always the case for the parameter sets used in this paper. It is convenient to introduce Λ as

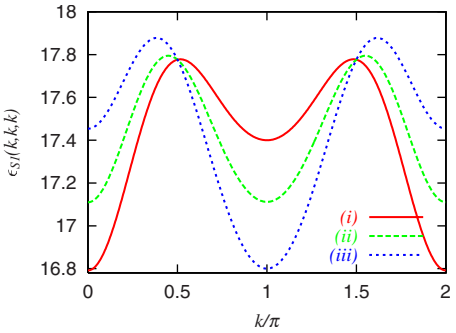

FIG. 5. (Color online) The dispersion relation of the excitation energy $\epsilon_{\mathrm{S1}}(\mathbf{k})$ for $\mathbf{k}=(k,k,k)$, $h=0$, $J_1^z=3$, $J_2^z=1$, and $J_1^{\perp}=-1$. (i) is obtained at $J_2^{\perp}=0.1$ and the minimum is at $\mathbf{k}=\mathbf{Q}_1$. (ii) is at $J_2^{\perp}=0.148$ and the minima are at both $\mathbf{k}=\mathbf{Q}_1$ and $\mathbf{Q}_2$. (iii) is at $J_2^{\perp}=0.2$ and the minimum is at $\mathbf{k}=\mathbf{Q}_2$.

$$\Lambda \equiv \epsilon_{\mathrm{S1}}^{(1)}(\mathbf{Q}_2)^2 - \epsilon_{\mathrm{S1}}^{(1)}(\mathbf{Q}_1)^2 = 16[-J_2^{\perp}(12J_1^z - 9J_2^z) + 4J_1^{\perp 2}], \tag{29}$$

Then, one chooses $\mathbf{k}=\mathbf{Q}_1$ when $\Lambda > 0$ or $\mathbf{k}=\mathbf{Q}_2$ when $\Lambda < 0$. We have checked that the SS with $\mathbf{Q}_1$ (SS1) is always favored for $J_2^{\perp} \le 0$. And when the Ising-like anisotropy is large, i.e., $12J_1^z - 9J_2^z \gg 4J_1^{\perp}$, very small positive $J_2^{\perp}$ selects the SS with $\mathbf{Q}_2$ (SS2). For each case, we plot the dispersion relation $\epsilon_{\mathrm{S1}}(\mathbf{k})$ along the (1,1,1) direction in Fig. 5.

From Eq. (18), the chemical potentials of both phases are given by

$$\mu_{\mathrm{S1SS}i} \equiv h - \epsilon_{\mathrm{S1}}(\mathbf{Q}_i), \quad \text{for } i=\{1,2\}, \tag{30}$$

where the subscript "Sn" means that the interactions are expanded up to n-th order in S^{-1} and "SSi" represents the types of the SS. The effective masses are isotropic and are respectively given by

$$m_{\mathrm{S1SS1}} = \frac{\sqrt{(4J_1^z - 3J_2^z + 3J_2^{\perp})^2 - 16J_1^{\perp 2}}}{2S\{-J_2^{\perp}(4J_1^z - 3J_2^z + 3J_2^{\perp}) + 4J_1^{\perp 2}\}}, \tag{31a}$$

$$m_{\mathrm{S1SS2}} = \frac{1}{2SJ_2^{\perp}}. \tag{31b}$$

When $\Lambda=0$, the two minima are degenerate and we have to take into account two independent condensates and phases which are not characterized by Eq. (17) may appear. A brief discussion on this case is given in Appendix A. The SS phase of four-sublattice structure (SS3) actually exists for certain parameter sets. There exist three types of SS around the half-filled solid.

Next, we consider the stability of the SS phase. The two-body interaction between α bosons is given by the first-order diagram since the bare Green's function of $\alpha(\beta)$ bosons is $i/(\omega - S\epsilon_{\alpha}^{(1)}(\mathbf{k}) \pm h) = O(S^{-1})$ for $\omega \sim -\mu_{\alpha}$ and the vertex function is $O(S^0)$. The alternative view is that, if we rescale the Hamiltonian by S^{-1}, the vertex function is $O(S^{-1})$ and the diagram is suppressed by S^{-1} for each vertex. Therefore, we need only the vertex function between α bosons. By replac-

ing $a_{\mathbf{k}} \to \cosh\theta_{\mathbf{k}}^{(1)}\alpha_{\mathbf{k}}$ and $b_{\mathbf{k}} \to -\sinh\theta_{\mathbf{k}}^{(1)}\alpha_{\mathbf{k}}^{\dagger}$ in H, the interaction term of α bosons appears as the following form:

$$\frac{1}{2N}\sum V_{\alpha}(\mathbf{q};\mathbf{k}_1,\mathbf{k}_2)\alpha_{\mathbf{k}_1+\mathbf{q}}^{\dagger}\alpha_{\mathbf{k}_2-\mathbf{q}}^{\dagger}\alpha_{\mathbf{k}_1}\alpha_{\mathbf{k}_2}, \tag{32}$$

where the factor 2 in front of N is considered for the symmetry factor. For the case $\Lambda>0$ and $\mathbf{Q}=\mathbf{Q}_1(=0)$, Γ is given by,

$$\Gamma_{\mathrm{S1SS1}} = V_{\alpha}(0;\mathbf{Q}_1,\mathbf{Q}_1) = 6(J_2^z - J_2^{\perp}), \tag{33}$$

Thus, SS phase of $\mathbf{Q}_1$ is stable for $J_2^z - J_2^{\perp} > 0$.

For the case $\Lambda<0$ and $\mathbf{Q}=\mathbf{Q}_2$, Γ is given by,

$$\Gamma_{\mathrm{S1SS2}} = V_{\alpha}(0;\mathbf{Q}_2,\mathbf{Q}_2) = 6(J_2^z + J_2^{\perp}), \tag{34}$$

In this phase, the Spin on B sublattice does not have the transverse magnetization even for $\mu_{\mathrm{S1SS2}}>0$ since $\sinh\theta_{\mathbf{Q}_2}^{(1)}=0$.

To see the validity of the above picture, we compare the above result with that of the MFT. Although there exists the extensive MFT calculation of this model for[8,9] $J_2^{\perp}<0$, to the best of our knowledge, there is not the appropriate mean-field calculation of the models for $J_2^{\perp}>0$. Hence, we redo the MFT for $S=1/2$. Now, the ground-state energy is obtained by replacing the operators in H with their expectation values of Pauli matrices on each site, e.g., $\Sigma_{\langle i,j\rangle}S_i^zS_j^z \to \Sigma_{\langle i,j\rangle}S^2\langle\sigma_i^z\rangle\langle\sigma_j^z\rangle$. We compare energies of the three types of spin configurations,

$$\frac{E_1^{\mathrm{mean}}}{NS^2} = 8J_1^z\langle\sigma^z\rangle\langle\sigma^z\rangle' + 3J_2^z(\langle\sigma^z\rangle^2 + \langle\sigma^z\rangle'^2) - 8|J_1^{\perp}|\tau\tau' + 3J_2^{\perp}(\tau^2+\tau'^2) + h(\langle\sigma^z\rangle + \langle\sigma^z\rangle'), \tag{35a}$$

$$\frac{E_2^{\mathrm{mean}}}{NS^2} = 8J_1^z\langle\sigma^z\rangle\langle\sigma^z\rangle' + 3J_2^z(\langle\sigma^z\rangle^2 + \langle\sigma^z\rangle'^2) - 3J_2^{\perp}(\tau^2+\tau'^2) + h(\langle\sigma^z\rangle + \langle\sigma^z\rangle'), \tag{35b}$$

$$\frac{E_{1/4\mathrm{filled}}}{NS^2} = -h. \tag{35c}$$

where $\tau=\sqrt{\langle\sigma^x\rangle^2+\langle\sigma^y\rangle^2}=\sqrt{1-\langle\sigma^z\rangle^2}$. E_1^{mean} is obtained from the two-sublattice structure, E_2^{mean} is from the two-sublattice structure of $\langle\sigma^z\rangle$ and τ with AF-(π,π,π) $\langle\sigma^{x,y}\rangle$ ordering on each sublattice, and $E_{1/4\mathrm{filled}}$ is from the quarter-filled solid. In this paper, we ignore the possibility that another types of SS phases appear around the quarter-filled solid as in the model on the square lattice.[12,31] By minimizing each energy numerically, we obtain magnetization curves for various parameters. We confirmed that the Bose-gas approach gives the same results as the MFT one. The specific examples are shown in Fig. 6.

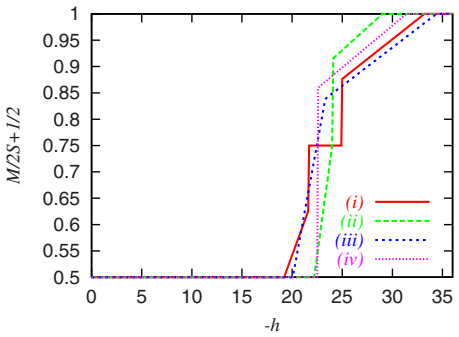

FIG. 6. (Color online) Magnetization curves obtained from the MFT for $J_1^z=3$, $J_1^{\perp}=-1$. We assume two-sublattice structure or the quarter-filled solid. M is given by $(1/2N)\Sigma_1^{2N}\langle S_{\mathbf{i}}^z\rangle$. (i) curve is obtained for $J_2^z=0.5$, $J_2^{\perp}=0.3$. (ii) is for $J_2^z=-0.1$, and $J_2^{\perp}=0.4$. (iii) is for $J_2^z=0$ and $J_2^{\perp}=-0.4$. (iv) is for $J_2^z=-0.5$ and $J_2^{\perp}=-0.4$. All curves has a half-filled solid around $h=0$ and SF phase below the saturation field. (i) curve has SS2 just ahead the half-filled solid, and the quarter-filled solid. (ii) has SS2 also. (iii) has SS1 which is connected to SF phase continuously. (iv) does not have SS phase.

B. Second-order perturbation

To see the effect of quantum fluctuation more clearly, we consider the second-order perturbation theory in the parameter S^{-1}. In this order, the ground-state phase may become different from the mean-field one.

To begin with, let us consider the state of the half-filled solid by diagonalizing the quadratic term in the Hamiltonian. When the interaction terms (8c) are written in terms of the Bogoliubov-transformed bosons and put into the normal-order form, additional quadratic terms appear. As a result, the quadratic part of Hamiltonian reads,

$$\begin{aligned} H_{\mathrm{quadS2}} = {} & \{(S\epsilon_0(\mathbf{k}) - T_1(\mathbf{k}))\cosh 2\theta_{\mathbf{k}} - (St_0(\mathbf{k}) \\ & - T_2(\mathbf{k}))\sinh 2\theta_{\mathbf{k}} - Sh\}\alpha_{\mathbf{k}}^{\dagger}\alpha_{\mathbf{k}} + \{(S\epsilon_0(\mathbf{k}) \\ & - T_1(\mathbf{k}))\cosh 2\theta_{\mathbf{k}} - (St_0(\mathbf{k}) - T_2(\mathbf{k}))\sinh 2\theta_{\mathbf{k}} \\ & + Sh\}\beta_{\mathbf{k}}^{\dagger}\beta_{\mathbf{k}} + \{-(S\epsilon_0(\mathbf{k}) - T_1(\mathbf{k}))\sinh 2\theta_{\mathbf{k}} + (St_0(\mathbf{k}) \\ & - T_2(\mathbf{k}))\cosh 2\theta_{\mathbf{k}}\}(\alpha_{\mathbf{k}}\beta_{\mathbf{k}} + \alpha_{\mathbf{k}}^{\dagger}\beta_{\mathbf{k}}^{\dagger}), \end{aligned} \tag{36}$$

where T_ks are given by Eq. (B1). Even in the normal-ordered two-body interaction terms, there exists the terms which shift the vacuum with respect to α and β (e.g., $\alpha^{\dagger}\beta^{\dagger}\alpha^{\dagger}\beta^{\dagger}|0\rangle \neq 0$), which leads to the self-energy. However, this contributes the Green's function in the third order of S^{-1} and we neglect the self-energy in our approximation. We note that, even if we use Holstein-Primakoff transformation, the same quadratic Hamiltonian is obtained up to the second order in S^{-1}. The difference between the two boson representations (i.e., Dyson-Maleev and Holstein-Primakoff) appears in the two-body interaction term.

Now, $\theta_{\mathbf{k}}$ is given by solving

$$[-S\epsilon_0(\mathbf{k}) + T_1(\mathbf{k})]\sinh 2\theta_{\mathbf{k}} + [St_0(\mathbf{k}) - T_2(\mathbf{k})]\cosh 2\theta_{\mathbf{k}} = 0. \tag{37}$$

To evaluate $T_{1,2}$, we need the explicit form of the function $\theta_{\mathbf{k}}$. Since $T_{1,2}$ is suppressed by a factor $1/S$ in the diagonalization procedure, we use $\theta_{\mathbf{k}}^{(1)}$ which is obtained in the first-order calculation for the integrands in Eq. (B1). Therefore, $\theta_k^{(2)}$ which is corrected up to second order is given by

$$\tanh 2\theta_k^{(2)} = \frac{t_0(\mathbf{k}) - T_2^{(1)}(\mathbf{k})/S}{\epsilon_0(\mathbf{k}) - T_1^{(1)}(\mathbf{k})/S}. \tag{38}$$

If $|\tanh 2\theta_k^{(2)}| > 1$, the spinwave expansion concludes that the half-filled solid is unstable and that other phases may take over. In fact, this happens for certain choices of the parameters. The detailed result will be discussed in Sec.VI. Then the quadratic Hamiltonian and the dispersion relation $\epsilon_{S2}(\mathbf{k})$ are given, respectively, by

$$H_0' = S[\epsilon_{S2}(\mathbf{k}) - h]\alpha_{\mathbf{k}}^\dagger \alpha_{\mathbf{k}} + S[\epsilon_{S2}(\mathbf{k}) + h]\beta_{\mathbf{k}}^\dagger \beta_{\mathbf{k}}, \tag{39}$$

$$\epsilon_{S2}(\mathbf{k}) = \sqrt{\left(\epsilon_0(\mathbf{k}) - \frac{T_1^{(1)}(\mathbf{k})}{S}\right)^2 - \left(t_0(\mathbf{k}) - \frac{T_2^{(1)}(\mathbf{k})}{S}\right)^2}. \tag{40}$$

If we introduce the appropriate constants $a_1, \ldots, a_3$, the above phonon dispersion $\epsilon_{S2}(\mathbf{k})$ may be written generally as:

$$\epsilon_{S2}(\mathbf{k}) = \sqrt{[a_1 + a_2 C_2(\mathbf{k})]^2 - [a_3 C_1(\mathbf{k})]^2}, \tag{41}$$

and qualitatively the same dependence on $\mathbf{k}$ as in the first-order case is obtained. In our calculations, the minimum is always locked at $\mathbf{Q}_1 = (0,0,0)$ or $\mathbf{Q}_2 = (\pi,\pi,\pi)$, which respectively corresponds to SS1 or SS2. The criterion, which determines the structure and the effective mass for each phase, is easily obtained in the same manner as in the first-order case [see Eq. (29) and (31)]. However, the explicit forms are somewhat lengthy and we do not show them in this paper. In the following, we shall concentrate on the physics of SS1 and SS2 and shall not discuss SS3 further. The chemical potential μ_α, which controls the onset of BEC, are also different from the first-order one (30) and is given by

$$\mu_{S2SSi} \equiv h - \epsilon_{S2}(\mathbf{Q}_i), \quad \text{for } i = \{1,2\}. \tag{42}$$

Next, we briefly recapitulate the method by which we calculate the effective interaction Γ among the condensed bosons. We simply evaluate the diagrams up to the second order in S^{-1}. We have one diagram at the first order and six at the second order. The second-order diagrams are shown in Fig. 7. To evaluate the second order diagram, we use the bare Green's function at $\mu_{S2SSi} = 0$ in the dilute-Bose-gas approximation:

$$\langle T(\alpha_k \alpha_k^\dagger)(\omega)\rangle = \frac{i}{\omega - S[\epsilon_{S2}(\mathbf{k}) - \epsilon_{S2}(\mathbf{Q}_i)] + i0^+}. \tag{43}$$

In the presence of a finite condensate $|\langle\alpha\rangle|^2 = \rho \propto \mu$, the Green's function, which is obtained for a operator $\alpha' = \alpha - \langle\alpha\rangle$, gets modified continuously from the one at the onset of BEC.[37] Specifically, $\langle\alpha'\alpha'^\dagger\rangle_{\text{at } \mu>0} = \langle\alpha\alpha^\dagger\rangle_{\text{at } \mu=0} + O(\mu)$, and $\langle\alpha'\alpha'\rangle_{\text{at } \mu>0} = O(\mu)$. In short, the modified quadratic Hamiltonian and the effective interaction Γ calculated above tell us the stability and the low-energy physics of solid and SS phase. The detailed results are shown in Sec. VI.

Finally, we consider the validity of the expansion of the exponential in powers of the interaction terms in the path integral when we calculate Γ. If we were able to take into account an infinite number of terms, the expansion would be correct. However, now we sum up only a finite number of terms. Thus, we need a criterion, even though naive, for determining the reliability of the expansion. A natural candidate may be the magnitude of the expanded interaction terms. To see this explicitly, we consider the following simple boson model on the simple cubic lattice:

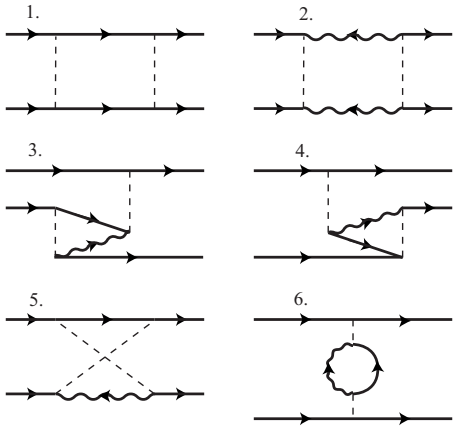

FIG. 7. The second-order (one-loop) diagrams in S^{-1}. Straight lines (wavy lines) denote $\alpha(\beta)$ bosons. Broken lines denote the momentum transfer at the interaction.

$$H_s = \sum_k \frac{\mathbf{k}^2}{2m} d_{\mathbf{k}}^\dagger d_{\mathbf{k}} + \frac{1}{2N} \sum_{\mathbf{k}_1,\mathbf{k}_2,\mathbf{q}} 2\lambda d_{\mathbf{k}_1+\mathbf{q}}^\dagger d_{\mathbf{k}_2-\mathbf{q}}^\dagger d_{\mathbf{k}_1} d_{\mathbf{k}_2} \tag{44}$$

In this model, the low-energy effective interaction Γ_s between the condensed bosons is exactly obtained as $\Gamma_s = 2\lambda/[1 + (2/\pi)m\lambda] = 2\lambda\Sigma_n[-(2/\pi)m\lambda]^n$. The dimensionless constant $m\lambda$ captures the magnitude of the expanded interaction terms. Thus, for general lattice boson models, we may expect that (mass) × (coupling constant) gives a simple criterion for the validity of the expansion.

Let us apply the above criterion to our case. For the boson masses, we use Eq. (31), which are correct up to the first order in S^{-1}, for simplicity. An appropriate choice of the coupling constants may be J_i^z and $J_i^\perp$ for $i = \{1,2\}$. For SS2, the criterion reads $J_i^z m_{2\text{cl}} = J_i^z/(2SJ_2^\perp)$. Hence, however large the spin S may be, the series expansion of Γ eventually diverges for relatively large Ising anisotropy. Similarly for SS1, the perturbation expansion is not converging for large Ising anisotropy since $m_{1\text{cl}} \sim -1/(2SJ_2^\perp)$. We have one more problem in the evaluation of Γ; when the energy dispersion at the solid is nearly gapless [i.e., $\tanh 2\theta_{\mathbf{k}=0} \approx 1$ in Eqs. (15) and (16)], $\cosh 2\theta_0$ and $\sinh 2\theta_0$ have large values(for $\tanh 2\theta \to 1$, $\theta \to \infty$). We note that these problems are peculiar to the evaluation of Γ and the low-energy physics of the solid (NAF) is well understood by the large-S expansion.

From the above discussion, we may conclude that the SS phases obtained within the MFT, which do not change even after the first-order $1/S$-correction is taken into account, might be destroyed at higher orders by quantum fluctuations. Since the perturbation expansion described above is ill behaved for large Ising anisotropy, we have to take another approach to closely investigate the fate of the SS phases. In the next section, we shall introduce another perturbation theory with respect to large Ising anisotropy. A reliable treat-

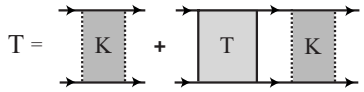

FIG. 8. Ladder diagram: T represents the ladder diagram and K represents the kernel which is not reducible to the product of two-particle Green's function.

ment of Γ for the case with $\tanh 2\theta_{\mathbf{k}=0} \approx 1$ remains to be an open problem.

V. PERTURBATION THEORY IN LARGE ISING-LIKE ANISOTROPY

In the limit $J_1^z \nearrow \infty$, the system behaves like the Ising model. In this section, we compute Γ by the perturbation theory in $(J_1^z)^{-1}$. Specifically, we develop an expansion in small coupling constants $(J_2^z, J_1^\perp, J_2^\perp)$.

A. First-order perturbation

If we diagonalize the bare quadratic Hamiltonian H_0 (8b),

$$\tanh 2\theta_{\mathbf{k}} = \frac{J_1^\perp C_1(\mathbf{k})}{4J_1^z - 3J_2^z + J_2^\perp C_2(\mathbf{k})} = O(1/J_1^z), \tag{45}$$

Then,

$$\cosh \theta_{\mathbf{k}} = 1 + O[(J_1^z)^{-2}], \quad \sinh \theta_{\mathbf{k}} = O[(J_1^z)^{-1}]. \tag{46}$$

If we assume that the exact $\theta_{\mathbf{k}}$ obtained by Eq. (16) has the same property, the self-energy contribution to the quadratic Hamiltonian $[\epsilon'(\mathbf{k}), t'(\mathbf{k})$ in Eq. (12)] is up to $O[(J_1^z)^0]$ and the dependence on J_1^z of $\theta_{\mathbf{k}}$ is maintained as Eq. (46). Therefore, the leading-order Hamiltonian in J_1^z reads

$$H_{\mathrm{I1}} = \sum_{\mathbf{k}} S[\epsilon_0(\mathbf{k}) - h]\alpha_{\mathbf{k}}^\dagger \alpha_{\mathbf{k}} + \sum_{\mathbf{k}} S[\epsilon_0(\mathbf{k}) + h]\beta_{\mathbf{k}}^\dagger \beta_{\mathbf{k}},$$

$$+ \frac{1}{N}\sum_{\mathbf{k}_1,\mathbf{k}_2,\mathbf{q}} [J_2^z C_2(\mathbf{q}) - J_2^\perp C_2(\mathbf{k}_2)]\alpha_{\mathbf{k}_1+\mathbf{q}}^\dagger \alpha_{\mathbf{k}_2-\mathbf{q}}^\dagger \alpha_{\mathbf{k}_1}\alpha_{\mathbf{k}_2}. \tag{47}$$

where we neglect the two-body interaction term containing β bosons since the gap of β boson is $O(J_1^z)$ when the gap of α boson closes. The meaning of the subscript "In" is similar to that of "Sn" in the previous section; it means that terms are kept up to n-th order in the Ising expansion. The minimum of the dispersion is obtained at $\mathbf{Q}_1 = (0,0,0)$ for $J_2^\perp < 0$ (SS1) or $\mathbf{Q}_2 = (\pi,\pi,\pi)$ for $J_2^\perp > 0$ (SS2). The chemical potential and the effective mass are respectively given by

$$\mu_{\mathrm{I1}} = h - (8J_1^z - 6J_2^z - 6|J_2^\perp|), \tag{48a}$$

$$m_{\mathrm{I1}} = \frac{1}{2S|J_2^\perp|}. \tag{48b}$$

Next, let us evaluate the interaction Γ among the α bosons. Since both the Green's function of α bosons and the coupling constants of interaction are $O[(J_1^z)^0]$, the all-order diagrams equally contribute to Γ, which is given by the ladder diagram (Fig. 8). The ladder diagram T evaluated at the solid satisfies

$$T(\mathbf{q};\mathbf{k}_1,\mathbf{k}_2) = K(\mathbf{q};\mathbf{k}_1,\mathbf{k}_2) - \frac{1}{N} \times \sum_{\mathbf{q}'} \frac{T(\mathbf{q}';\mathbf{k}_1,\mathbf{k}_2)K(\mathbf{q}-\mathbf{q}';\mathbf{k}_1+\mathbf{q},\mathbf{k}_2-\mathbf{q})}{\omega(\mathbf{k}_1+\mathbf{q}') + \omega(\mathbf{k}_2-\mathbf{q}') - \omega(\mathbf{k}_1) - \omega(\mathbf{k}_2)}. \tag{49}$$

where the particle corresponding to the external line is assumed to be a real one with the energy $\omega(\mathbf{k}) - \mu$. One obtains the parameter Γ for $\mathrm{SS}_i(\mathbf{Q}_i)$ as $\Gamma_{\mathrm{SS}_i} = T(0,\mathbf{Q}_i,\mathbf{Q}_i)$.

Now, the kernel K and the energy ω are given by

$$K_{\mathrm{I1}}(\mathbf{q};\mathbf{k}_1;\mathbf{k}_2) = 2J_2^z C_2(\mathbf{q}) - J_2^\perp[C_2(\mathbf{k}_1) + C_2(\mathbf{k}_2)], \tag{50a}$$

$$\omega_{\mathrm{I1}}(\mathbf{k}) = 2S[J_2^\perp C_2(\mathbf{k}) + 3|J_2^\perp|]. \tag{50b}$$

The self-consistent Eq. (49) for the ladder diagram is exactly solvable[21,22] and we obtain

$$\Gamma_{\mathrm{I1SS}_i} = \frac{6(J_2^z + |J_2^\perp|)}{1 + 0.258\dfrac{(J_2^z + |J_2^\perp|)}{S|J_2^\perp|}}, \tag{51}$$

for $i = \{1,2\}$. If the limit $S \to \infty$ is taken, Γ reduces to the first-order result in the large-S expansion [Eqs. (33) and (34)]. For finite S, Γ is suppressed by quantum fluctuations. However, concerning the stability of the SS phases, there is no difference from the MFT result as far as the denominator is positive. We note that if

$$1 + 0.258\frac{(J_2^z + |J_2^\perp|)}{S|J_2^\perp|} = 0, \tag{52}$$

the effective interaction Γ_{I1SS_i} diverges. This suggests the possibility of the SS accompanied by the bound-magnon BEC. A brief discussion on this issue will be given in Sec. V C.

B. Second-order perturbation

In this section, we study the SS phase around the solid in the second-order perturbation in $(J_1^z)^{-1}$ with the help of large S expansion.

To obtain the renormalized quadratic Hamiltonian, we perform the Bogoliubov transformation and normal-order the interaction term, sorting out the terms based on Eq. (46). Since near the boundary of NAF-CAF transition quantum fluctuation may play an important role, we keep only terms of order $O(J_2^z/(J_1^z)^2)$ [we neglect the order $O[(J_2^z/J_1^z)^n/J_1^z]$ terms with $n \geq 2$]. Even on the classical boundary, $6J_2^z = (1/2)8J_1^z$ and the J_2^z times coordination number is suppressed by the large-anisotropy J_1^z. Therefore, the expansion may work. Since the renormalized $\theta_{\mathbf{k}}$ satisfies Eq. (46), the off-diagonal part of quadratic Hamiltonian is given by

$$H_{(\mathrm{I2})\mathrm{off}} = \sum_{\mathbf{k}} \left\{ S[-\epsilon_0(\mathbf{k})\sinh 2\theta_{\mathbf{k}} + t_0(\mathbf{k})\cosh 2\theta_{\mathbf{k}}] + \frac{J_1^z}{2}\left[\frac{1}{N}\sum_{\mathbf{q}} C_1(\mathbf{q})\sinh\theta_{\mathbf{q}}\right] C_1(\mathbf{k}) \right\} (\alpha_{\mathbf{k}}\beta_{-\mathbf{k}} + \alpha_{\mathbf{k}}^\dagger \beta_{-\mathbf{k}}^\dagger). \tag{53}$$

Now, approximately $\sinh\theta_{\mathbf{k}} = t_0(\mathbf{k})/2\epsilon_0(\mathbf{k}) + \Delta_{\mathbf{k}}$, where $\Delta_{\mathbf{k}}$ is $O(J_1^{z-1})$. Then, the leading order of $\Delta_{\mathbf{k}}$ is obtained and, as a result, $\theta_{\mathbf{k}}$ is given by

$$\sinh\theta_{\mathbf{k}}^{(\mathrm{I2})} = A_1 C_1(\mathbf{k}), \tag{54a}$$

$$\cosh\theta_{\mathbf{k}}^{(\mathrm{I2})} = 1 + \frac{A_1^2}{2} C_1(\mathbf{k})^2, \tag{54b}$$

where

$$A_1 = \frac{2J_1^\perp S}{4S(4J_1^z - 3J_2^z) - J_1^z}. \tag{55}$$

Now, the quadratic part of the Hamiltonian reads

$$H_{(\mathrm{I2})0} = \sum_{\mathbf{k}} [\epsilon_{\mathrm{I2}}(\mathbf{k}) - h]\alpha_{\mathbf{k}}^\dagger \alpha_{\mathbf{k}} + [\epsilon_{\mathrm{I2}}(\mathbf{k}) + h]\beta_{\mathbf{k}}^\dagger \beta_{\mathbf{k}}, \tag{56}$$

where

$$\epsilon_{\mathrm{I2}}(\mathbf{k}) = 8SJ_1^z - 6SJ_2^z - 16J_1^z A_1^2 + 12J_2^z A_I^2 + (2SJ_2^\perp + 2J_2^z A_1^2) C_2(\mathbf{k}) + [2(8SJ_1^z - 6SJ_2^z - J_1^z)A_1^2 - 4SJ_1^\perp A_1] C_1(\mathbf{k})^2. \tag{57}$$

Then, the minimum of dispersion is obtained at $\mathbf{Q}_1 = (0,0,0)$ or $\mathbf{Q}_2 = (\pi,\pi,\pi)$ as in the first-order result. The chemical potentials and the effective masses for each phase are given by the same way as in Sec. IV A; [see Eqs. (30) and (31)].

Let us evaluate the two-body interaction Γ between the condensed bosons. As in the first-order case in $1/J_1^z$, we need to calculate the kernel in the ladder diagram (see Fig. 8). When the gap of the α boson closes, that of the β bosons is $O(J_1^z)$. Then, the correlation of the β boson remains short-ranged for low energies and $\langle T(\beta_{\mathbf{k}}\beta_{\mathbf{k}}^\dagger)(E \approx 0)\rangle = O(1/J_1^z)$. The effect of β operator in the interaction term is at most $O(1/\sqrt{J_1^z})$. Therefore, the interaction part of the Hamiltonian which affects the kernel is obtained and is given in Eq. (B2). Now, we shall evaluate the kernel. Before doing so, a remark is in order; at the second order of $1/J_1^z$ an infinite number of diagrams appear in the kernel. Hence, with the help of large S expansion, we keep the term of the third order of S (up to two-loop diagrams) and neglect the term of $O[(J_1^z)^{-1}S^{-3}]$. In the selection of diagrams which contribute to the kernel, we do not view J_2^z as a special contrary to the case of the quadratic Hamiltonian, for simplicity. As a result, in the second order of S, four diagrams and, in the third order of S, fourteen diagrams contribute to the kernel. The one-loop diagrams are given by $3 \sim 6$ shown in Fig. 7, and the part of the two-loop diagrams are shown in Fig. 9. When we evaluate the diagrams, we drop the term of $O[(J_1^z)^{-2}]$ after the frequency of the propagator is integrated out. In this calculation, we maintain the terms J_2^z which are readily obtained in the quadratic Hamiltonian, even if the contribution of these term is $O[J_2^z(J_1^z)^{-2}]$. Concretely, we use the gap of β boson as $2S(8J_1^z - 6J_2^z)$ and maintain J_2^z of Eqs. (55) and (57). We solve Eq. (49) by substituting the obtained kernel, and the interaction Γ between condensed bosons is obtained. The detailed results are shown in Sec. VI.

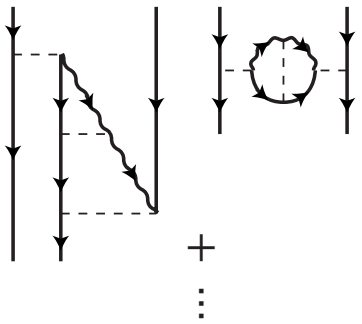

FIG. 9. The part of two-loop diagrams which contributes to the kernel in the order in $S^{-2}(J_1^z)^{-1}$. Straight lines (wavy lines) denote $\alpha(\beta)$ boson. Broken lines denote the momentum transfer at the interaction.

C. Possibility of bound-magnon BEC

We briefly comment on the possibility of stable bound states. From the viewpoint of the Bethe-Salpeter equation, the two-particle Green's function contains the ladder diagram and the divergence of Γ implies the existence of stable bound states. In fact, this method has been successfully applied[23,24] to search for the stable bound-magnon state in the vicinity of the saturated ferromagnetic phase of one-dimensional and 3D frustrated magnets. Hence, the above ladder approximation may be also applied to study the bound-magnon BEC around the solid. Now, we note that within the first-order perturbation the effective interaction Γ_{I1SS_i} [Eq. (51)] diverges when

$$1 + 0.258\frac{(J_2^z + |J_2^\perp|)}{S|J_2^\perp|} = 0. \tag{58}$$

In fact, we found that Γ had a pole below the two-particle threshold when the left-hand side of Eq. (58) is negative. Therefore, when the denominator of Eq. (51) is equal to 0 or negative, we may expect that, instead of the usual magnons, the bound magnon condenses at the center-of-mass momentum $\mathbf{K}=0$ provided that the chemical potential is properly tuned. We found that the energy of the bound state at $\mathbf{K} = (\pi,\pi,\pi)$ is higher in energy than the one at $\mathbf{K}=0$ and will not affect the critical value of μ (or h) at which the bound-magnon BEC occurs. However, the extensive studies on hardcore Bose Hubbard models by quantum Monte Carlo simulations[10–12,26–28] have never indicated the existence of an SS accompanied by a bound-magnon BEC. Hence, it would be useful to reconsider this problem from the energetic point of view, even though rough.

Of course, some other phases may compete with the bound-magnon phase. In particular, the SF phase, which may

appear from the solid phase via the first-order transition, would be an important candidate. In the MFT, a solid-superfluid (S-SF) transition occurs at

$$h_{\text{S-SF}} = 2\sqrt{16J_1^{z2} - (3J_2^z + 4|J_1^\perp| - 3J_2^\perp)^2} = 8J_1^z - |O(J_1^{z-1})|. \tag{59}$$

From (48a), on the other hand, one sees that the bound-magnon BEC starts at $h_b \approx 8J_1^z - 6(J_2^z + |J_2^\perp|) = 8J_1^z + O[(J_1^z)^0]$ when Eq. (58) is satisfied. In the case of the attraction $(J_2^z + |J_2^\perp|) < 0$, one sees that $h_b > h_{\text{S-SF}}$ and that a direct first-order S-SF transition occurs before the condensation of bound magnons. Hence, although an exotic SS phase brought about by the bound-magnon BEC may be expected (note that the gap of a bound magnon closes earlier than that of a *single* magnon) in the vicinity of the solid phase, what we actually have is a phase separation.

Therefore, in order to see the bound-magnon BEC around the half-filled solid, it may be necessary that higher-order terms in the perturbation in $1/J_1^z$ shift the critical value μ by $O[(J_1^z)^0]$. In this case, the approximation used in this section is beyond the scope of application to search the bound-magnon BEC. We do not go into more detailed discussion about the bound-magnon BEC in this paper.

VI. PHASE DIAGRAM

In Secs. IV and V, we have described the two methods of calculating the minimum **Q** of the dispersion by which the spin structure of the SS phase has been determined. On top of it, the mass, the chemical potential, and the interaction Γ which determines the stability of the SS have been computed. In this section, we show the detailed results on the phase diagram paying particular attention to the parameter set (3).

A. Stability of a half-filled solid—a spinwave analysis

The solid phase is stable when the energy gap is finite. Quantum fluctuations shift the energy gap and, in certain cases, the gap may close. In this subsection, we study the properties of the half-filled solid by the conventional spin-wave theory up to the second order in S^{-1}. Even for $S=1/2$, the approximation may work since the ground state is ordered.

At the first order in S^{-1}, the energy gap closes even at $h=0$ when $|\tanh \theta_{\mathbf{k}=0}^{(1)}| = 1$, and then the energy of the solid and the SF phase (or, a phase with magnetic long-range order in the xy plane) is degenerate within the MFT [see Eqs. (4), (5), and (26)]. For $|\tanh \theta_{\mathbf{k}=0}^{(1)}| > 1$, the SF phase is stabilized. In the second order in S^{-1}, the quantum fluctuation shift $\theta_{\mathbf{k}}^{(1)}$ to $\theta_{\mathbf{k}}^{(2)}$ and the boundary where the gap closes also changes. If the transition is a usual second-order one, the emergent phase may be SS. The first-order transition to the SF near the boundary may be also expected. However, in the case of 2D square lattice, the quantum Monte Carlo simulations indicate that at the Mott-SF transition point, $SU(2)$ symmetry dramatically restores[11] as in the classical case. Even though there exists the difference of the dimensionality, we may not exclude the possibility that on the phase boundary $SU(2)$ symmetry restores.

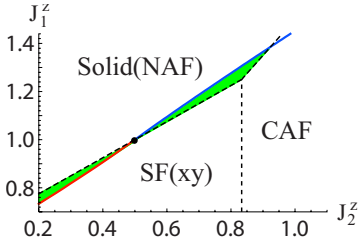

FIG. 10. (Color online) Phase boundary between the half-filled solid (or, the Ising-like NAF phase) and the SF phase (or, a phase with magnetic long-range order in the xy plane) obtained by the large-S expansion up to the order of S^0. Te values $S=1/2$, $J_1^\perp = 1$, $J_2^\perp = 0.5$, and $h=0$ (half-filled) are used. The solid line (blue) for $J_2^z \geq 0.5$ denotes the boundary where the gap of the solid phase closes. The solid line (red) for $J_2^z \leq 0.5$ denotes the boundary where the gap of the massive mode of the SF phase closes. The broken line (black) denotes the classical boundary between NAF, CAF, and SF phases. The dot represents the $J_1^z = 1$ and $J_2^z = 0.5$, where the system has $SU(2)$ symmetry and the boundaries intersect. In the highlighted region (green), the dispersion has a nonzero imaginary part and is ill-defined. For $J_2^z \geq 0.5$, the emergent phase may be either the SF or the SS. For $J_2^z \leq 0.5$, the emergent phase may be either the solid or the SS.

To see the properties of the resultant phases more clearly, we carry out the Holstein-Primakoff transformation starting from the SF phase (the xy-ordered NAF phase in the spin language) for $J_1^\perp > 0$ and calculate the magnon dispersion relation in the SF up to the second order in S^{-1} at $h=0$.

Let us briefly discuss some technical aspects of the calculation. There are two types of excitations: one is the gapless Goldston mode and the other is a massive (gapped) mode. To obtain these, we need to integrate out the functions of $\theta_{\mathbf{k}}$ as in Eq. (B1). If we substitute the $\theta_{\mathbf{k}}$ obtained in the first order as in Sec. IV B, the gapless Goldston mode remains gapless. As is well known, the spin-wave expansion is well-behaved if the ground state is classically stable. Hence, we do not extend the calculation to the region where the corresponding phase is unstable in the MFT. Concerning the gapped mode, when the gap closes at the first order in S^{-1}, the solid and the SF are degenerate in energy within the MFT. Since the gap of this mode is affected by the quantum fluctuations, the phase boundary is shifted in the second order in S^{-1}. The resulting phase may be either the solid or the SS phase.

As a result, a shift of the phase boundary is found in each phase, as is shown in Figs. 10 and 11. As has been discussed above, since the spin-wave expansion is well-behaved in the case that the selected phase is the classical ground state, only on the classical phase boundary, we can compare the dispersion of each phase explicitly. At the first order in S^{-1}, both dispersions are gapless. At the second order in S^{-1}, when the dispersion of one phase (solid or SF) is ill-defined, that of the other phase obtains the finite gap. If the system has the global $SU(2)$ (rotation) symmetry, the dispersion remains gapless. As a result, the shifted boundary forms the almost straight line which intersects that of the MFT at the parameter set where $SU(2)$ symmetry exists.

Next, let us discuss the application to ^{4}He as the QGM. As shown in Fig. 11, at the LF point, the solid phase is

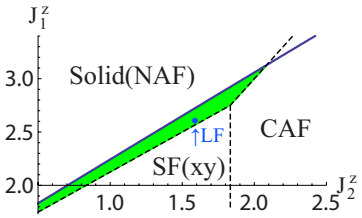

FIG. 11. (Color online) Phase boundary obtained by the large-S expansion up to the order of S^0 between the half-filled solid and the SF phase for $S=1/2$, $J_1^\perp=-1$, $J_2^\perp=-0.5$, and $h=0$ (half-filled). The solid line (blue) denotes the boundary where the gap of the solid phase closes. The broken line (black) denotes the classical boundary between NAF, CAF, and SF phases. The dot labeled as LF (blue) represents the LF point (3), which is suggested for the fitting parameters[9] of ^{4}He. In the highlighted region (green), the spin-wave expansion is ill-defined and the emergent phase may be either the SF or the SS. The straight line and the broken line intersect at $J_1^z=1$ and $J_2^z=-0.5$, where $SU(2)$ symmetry exists.

unstable even at $h=0$ and the resulting phase may be either the SF or the SS. To conjecture this phase, we plot the $\tanh\theta_{\mathbf{k}=0}$ of the massive modes as shown in Fig. 12. If $|\tanh\theta_{\mathbf{k}=0}|=1$, the energy gap closes. With the help of the fitting line, we see that on the parameters (3), the SF phase may be stabilized. Hence, on this parameter set, the QGM does not make a sense, and the fitting parameters for ^{4}He must be reconsidered by taking into account the quantum fluctuation.

B. Stability of supersolid

The fitting parameters for ^{4}He shall shift from Eq. (3). Although the shift may be quantitatively large to see Fig. 12, that is still expected to be perturbative since the quantum fluctuation is treated as a perturbation. Then, since the effective interaction Γ obtained within the first order in S^{-1} (or the

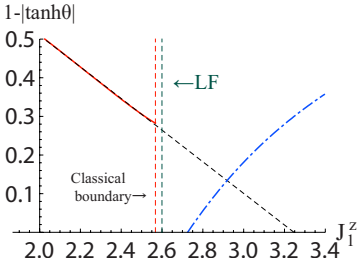

FIG. 12. (Color online) $1-|\tanh\theta^{(2)}_{\mathbf{k}=0}|$ obtained of the order of S^0 for $S=1/2$, $J_2^z=1.59$, $J_1^\perp=\pm1$, and $J_2^\perp=-0.5$ plotted as a function of J_1^z. If $1-|\tanh\theta^{(2)}_{\mathbf{k}=0}|=0$, the gap closes. The solid line (red) is given by the massive mode on the SF. We obtained it for $J_1^\perp=1$, which transforms to $J_1^\perp=-1$ by the gauge transformation. The dashed line (blue) is obtained on the solid phase. The vertical line labeled as LF represents the LF point (3). On the classical boundary, the gap of the SF phase largely opens. If we introduce the fitting line (the nonlabeled broken line), the gap of the SF phase seems to be open on the LF point and the stability of the SF is implied. Moreover, the gap seems to be maintained over the point where the gap of the solid phase closes. Hence, the solid-SF first-order transition is expected at $2.7\lesssim J_1^z\lesssim3.2$.

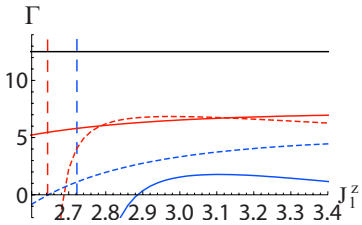

FIG. 13. (Color online) The interaction Γ for $J_2^z=1.59$, $J_1^\perp=-1$, and $J_2^\perp=-0.5$. Solid lines are obtained in the second order in S^{-1}. The broken lines are in the second order in $(J_1^z)^{-1}$. The curves are obtained, respectively, for $S=\infty$ (black), 1 (red), and 1/2 (blue) beginning at the top. The left vertical line (red) is the phase boundary for $S=1$ where the gap closes in the second order in S^{-1} at $h=0$. The right vertical line (blue) is for $S=1/2$. Near the boundary and for large J_1^z, the difference becomes large. For the large Ising-like anisotropy J_1^z, the evaluation of Γ in the second order in S^{-1} becomes pathologic as discussed in the last part of Sec. IV B

MFT) on Eq. (3) is robust [see Eq. (33)], the perturbative shift of the fitting parameters shall not affect the stability of the SS within the MFT. Therefore, we study the quantum effect to the stability of the SS near the LF point (3) by the Γ obtained in the second-order perturbation in S^{-1} and $1/J_1^z$. The repulsive nature of the effective interaction $\Gamma(>0)$ suggests the stability of the SS phase.

Since $J_1^\perp/J_2^\perp$ is fixed at 1/2 in the QGM, we plot Γ as a function of J_1^z and J_2^z, as is shown in Figs. 13 and 14. On the phase boundary, the perturbation theory in S^{-1} gives the divergence to $-\infty$ because of $\theta_{\mathbf{k}}$ for $\tanh\theta_{\mathbf{k}=0}\to1$ and the used approximation is beyond control. Near Eq. (3), the perturbation theory in $1/J_1^z$ also has the problem of accuracy since the suppression of the expansion parameter $1/J_1^z$ may not be sufficient. However, both methods lead to the one identical conclusion. In the case of $S=1/2$, both predict that Γ is considerably suppressed near Eq. (3), and, as a result, the second-order term has the same magnitude as the relatively large first-order term. Hence, quantitatively, it may be understood that the Γ of the MFT (that of the first order in S^{-1}) is not reliable near Eq. (3) and there exists the possibility that the quantum fluctuation breaks the stability of the SS. Therefore, even if the shift of the parameter set from Eq. (3) is

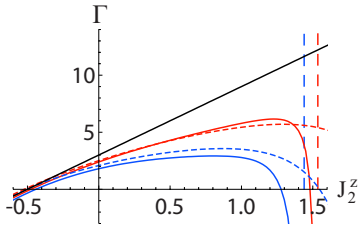

FIG. 14. (Color online) The interaction Γ for $J_1^z=2.60$, $J_1^\perp=-1$, and $J_2^\perp=-0.5$. Solid lines are obtained in the second order in S^{-1}. The broken lines are in the second order in $(J_1^z)^{-1}$. The curves are obtained, respectively, for $S=\infty$ (black), 1 (red), and 1/2 (blue) beginning at the top. The right vertical line (red) is the phase boundary for $S=1$ where the gap closes in the second order in S^{-1} at $h=0$. The left vertical line (blue) is for $S=1/2$. The shift of the boundary near $J_2^z=-0.5$ which determines the stability of the SS is extremely small and is within the error of $O(S^{-2})$ or $O((J_1^z)^{-2})$.

TABLE II. Types of phase transitions suggested by the several methods in this paper. "SW" and "Ising" represent the spinwave- and the Ising expansion discussed in Secs. IV and V, respectively. The interactions $\Gamma_{S1SSi}(i=1,2)$ and Γ_{I1SS_i} are given in Eqs. (33), (34), and (51), respectively. Γ_{S2SSi} and Γ_{I2SS_i} are shown in Figs. 13 and 14. If Γ diverges, one should not take the value literally, since even in that case a second-order solid-"bound-magnon SS (BMSS)" transition may be expected. The detailed discussion on a BMSS is given in Sec. V C.

Method	Solid SF	Solid SS	Solid BMSS
SW 1st	1st ($\Gamma_{S1SSi}<0$)	2nd ($\Gamma_{S1SSi}>0$)	
SW 2nd	1st ($\Gamma_{S2SSi}<0$)	2nd ($\Gamma_{S2SSi}>0$)	
Ising 1st	1st ($\Gamma_{I1SS_i}<0$)	2nd ($\Gamma_{I1SS_i}>0$)	2nd
Ising 2nd	1st ($\Gamma_{I2SS_i}<0$)	2nd ($\Gamma_{I2SS_i}>0$)	2nd
MFT	1st	2nd	

perturbative, the stability of the SS phase of ^{4}He remains to be a question.

Finally, we comment on the shift of the boundary which determines the stability of the SS given by the MFT. As is seen in Fig. 14, the quantum effect to Γ is very little on this boundary and the shift is within the error of approximation for both approximation $[O(S^{-2})$ or $O[(J_1^z)^{-2}]]$. We found that this is also the case for the SS2 which mainly appears for $J_2^\perp>0$ unless the parameter set sits near the phase boundary of solid SF at half filling. Therefore, if the energy of the solid phase is sufficiently less than the superfluid phase at half filling, the boundary determining the stability of the SS phase given by the MFT may not be affected by the quantum fluctuation.

VII. SUMMARY

By using the spin-wave $(1/S)$ and the Ising expansion together with the dilute-Bose-gas technique, we studied the SS phase around the half-filled solid (NAF) phase. First, we introduced two kinds of magnon excitations for the two sublattices in the NAF phase. At a certain value of chemical potential (or, the external magnetic field), the gap of one of the Bogoliubov-transformed magnons closes; this magnon BEC keeps the two-sublattice NAF structure intact implying the SS phase. The spin configuration of the SS phase was determined by the minimum of the energy spectrum over the solid ground state. The Bogoliubov-transformed magnons can be viewed as vacancies or interstitials introduced in solids. If the effective interaction Γ among the condensed magnons are repulsive, we may expect, on physical grounds, a stable SS phase to appear. Therefore, the necessary condition for a second-order solid-SS transition is given by $\Gamma>0$; if this condition is met, the SS phase realizes for low condensate density.

To evaluate the excitation spectrum in the solid phase and the effective interaction Γ in a quantum-mechanical manner, we developed the perturbation theory in S^{-1} and $(J_1^z)^{-1}$ in Secs. IV and V, respectively. (Table II)

The first-order calculation in S^{-1} yielded the same results as in the MFT; three types of SS phases are found around the half-filled solid. At the second order in S^{-1}, we found a possibility that quantum fluctuations destabilize the NAF solid, which is expected to be stable from the MFT. Specifically, in the evaluation of Γ, the second-order correction in S^{-1} becomes ill-behaved when the Ising-like anisotropy J_1^z is large or when the energy of the solid is almost the same as that of the SF at half filling. In such cases, the MFT (or, equivalently, the first-order perturbation in S^{-1}) may not be reliable.

In order to overcome this difficulty, we carried out another perturbation theory from the Ising limit (i.e., expansion in $1/J_1^z$). At the first order in $1/J_1^z$, we used the ladder approximation and saw that quantum fluctuations did suppress Γ, while we obtained the same result as the MFT one as far as the stability of the SS phase is concerned.

For negative Γ (i.e., attraction), we found a possibility of a phase characterized by the bound-magnon condensate. However, this phase may be replaced by the SF for the parameters considered in the text. In carrying out the second-order calculation in $1/J_1^z$, we used the ladder approximation with only diagrams up to two-loop (i.e., up to the third order in S^{-1}) kept in the kernel. The effect of quantum fluctuations depends crucially on the energies of the solid and the SF phase, as in the large-S expansion.

When the energy of the solid is sufficiently smaller than that of the SF phase at half filling, the second-order term had little effect on Γ in the vicinity of the MFT boundary (see Fig. 14). In other words, under the above condition, we may conclude that quantum fluctuations only have minor effects on the stability of the SS phase.

On the other hand, when the energy of the solid phase is comparable to that of the SF phase, there exists a possibility that quantum fluctuations completely wash out the SS phase obtained in the MFT. Actually, in the vicinity of the LF point, where frustration due to the competition among NAF, CAF and SF is strong, the second-order Ising-like expansion also concluded divergingly large negative values of Γ (see Figs. 13 and 14).

In Sec. VI, we studied the effect of quantum fluctuations on the ground state at the LF point. At the second order in S^{-1}, the ground state may be given not by the SS but by the SF even at $h=0$. The failure of the Liu-Fisher values to describe ^{4}He suggests that the optimal parameters, which should be obtained by fully quantum treatment, may differ from the Liu-Fisher ones. We expect that the deviation from the LF point is small and that it can be handled in a perturbative fashion. On the basis of this expectation, we studied the stability of the SS in the vicinity of the LF point. Since the energies of SS and SF are comparable in this region, the MFT may not be reliable. Even if the shift of the fitting parameters from the LF point is small and the MFT guarantees the stability of the SS, there remains a possibility that quantum fluctuations destabilize the SS. To investigate this possibility more closely, we shall need such a sophisticated treatment that the renormalization of the effective interaction Γ due to higher-order terms is appropriately taken into account.

Note added. After the completion of our work, we became aware of a series of papers by Stoffel and Gulácsi who studied the same model[38] as ours by the Green's function theory with the random-phase approximation. They reached a dif-

ferent conclusion that the critical external field at the solid-SS transition is little affected by quantum fluctuations at the LF point. We suspect that the discrepancy might be attributed to the difference in the approximation schemes; we believe that our approximation is well controlled by the two small parameters.

ACKNOWLEDGMENTS

We thank T. Momoi, N. Shannon, and D. Yamamoto for useful discussions and helpful correspondences. H.T.U is grateful to the hospitality of Condensed Matter Theory Laboratory and the financial support from the Junior Research Associate program at RIKEN. The author (K.T.) was supported by Grant-in-Aid for Scientific Research (C) Grant No. 20540375 and that on Priority Areas "Novel States of Matter Induced by Frustration" (Grant No. 19052003) from MEXT, Japan. This work was also supported by the Grant-in-Aid for the Global COE Program "The Next Generation of Physics, Spun from Universality and Emergence" from MEXT of Japan.

APPENDIX A: SUPERSOLID PHASE EMERGING FROM TWO TYPES OF BOSONS

In Sec. IV A, we have discussed the two SS phases, which are described by a single Boson condensate, and classified them by Λ (29). As has been mentioned there, however, in the case of $\Lambda=0$, the spin-wave dispersion takes its minima at both $\mathbf{Q}_1=(0,0,0)$ and $\mathbf{Q}_2=(\pi,\pi,\pi)$, and there exists a possibility that both kinds of bosons condense *simultaneously*. In this appendix, we discuss this possibility within the first-order perturbation in S^{-1}. We shall see that a new type of SS phase (SS3) appears for a certain parameter region; it has a four-sublattice structure and may continue to the quarter-filled solid.

As in the case of magnon BEC just below the saturation field,[22,24,25] the ground-state energy density may be expanded in powers of the boson densities;

$$\frac{E_{\mathrm{eff}}}{N} \approx \mathrm{const} + \frac{1}{2}\Gamma_{\mathbf{Q}_1}\rho_{\mathbf{Q}_1}^2 + \frac{1}{2}\Gamma_{\mathbf{Q}_2}\rho_{\mathbf{Q}_2}^2 + \Gamma_2\rho_{\mathbf{Q}_1}\rho_{\mathbf{Q}_2} + \Gamma_3\rho_{\mathbf{Q}_1}\rho_{\mathbf{Q}_2}\cos 2(\varphi_{\mathbf{Q}_1}-\varphi_{\mathbf{Q}_2}) - S\mu_0(\rho_{\mathbf{Q}_1}+\rho_{\mathbf{Q}_2}), \tag{A1}$$

where

$$\Gamma_2 = [V_\alpha(0;\mathbf{Q}_1,\mathbf{Q}_2) + V_\alpha(\mathbf{Q}_2-\mathbf{Q}_1;\mathbf{Q}_1,\mathbf{Q}_2) + V_\alpha(0;\mathbf{Q}_2,\mathbf{Q}_1) + V_\alpha(\mathbf{Q}_1-\mathbf{Q}_2;\mathbf{Q}_2,\mathbf{Q}_1)]/2,$$

$$\Gamma_3 = V_\alpha(\mathbf{Q}_2;\mathbf{Q}_1,\mathbf{Q}_1)[=V_\alpha(\mathbf{Q}_2;\mathbf{Q}_2,\mathbf{Q}_2)], \tag{A2}$$

and $\langle\alpha_q\rangle=\sqrt{N\rho_q}e^{i\varphi_q}$, $\Gamma_{\mathbf{Q}_j}=\Gamma_{\mathrm{S1SSj}}$ for $j=1,2$ [Eqs. (33) and (34)]. Since the Hamiltonian (8) is not hermitian, it is not always true that $V_\alpha(\mathbf{Q}_2;\mathbf{Q}_1,\mathbf{Q}_1)=V_\alpha(\mathbf{Q}_2;\mathbf{Q}_2,\mathbf{Q}_2)$. However, these coincides with each other when $\Lambda=0$. The relative angle $(\varphi_{\mathbf{Q}_1}-\varphi_{\mathbf{Q}_2})$ takes $0(\pi/2)$ when $\Gamma_3<0(>0)$.

If $\Gamma_{\mathbf{Q}_i}<0$ or $\sqrt{\Gamma_{\mathbf{Q}_1}\Gamma_{\mathbf{Q}_2}}<-(\Gamma_2-|\Gamma_3|)$, a magnetization jump occurs. Otherwise, when $\mathrm{Min}[\Gamma_{\mathbf{Q}_1},\Gamma_{\mathbf{Q}_2}]<\Gamma_2-|\Gamma_3|$, only one of the two species, which has smaller $\Gamma_{\mathbf{Q}_i}$ condenses and forms the spin structure (20). If $\mathrm{Min}[\Gamma_{\mathbf{Q}_1},\Gamma_{\mathbf{Q}_2}]>\Gamma_2-|\Gamma_3|$, Eq. (A5) takes the minimum when

$$\rho_{\mathbf{Q}_1} = \frac{\Gamma_{\mathbf{Q}_2}-(\Gamma_2-|\Gamma_3|)}{\Gamma_{\mathbf{Q}_1}\Gamma_{\mathbf{Q}_2}-(\Gamma_2-|\Gamma_3|)^2}S\mu_0,$$

$$\rho_{\mathbf{Q}_2} = \frac{\Gamma_{\mathbf{Q}_1}-(\Gamma_2-|\Gamma_3|)}{\Gamma_{\mathbf{Q}_1}\Gamma_{\mathbf{Q}_2}-(\Gamma_2-|\Gamma_3|)^2}S\mu_0. \tag{A3}$$

Then, the spin configuration is given by,

$$\langle S_l^x\rangle = \sqrt{2S}[\sqrt{\rho_{\mathbf{Q}_1}}\cosh\theta_{\mathbf{Q}_1}^{(1)}\cos\varphi_{\mathbf{Q}_1} + \sqrt{\rho_{\mathbf{Q}_2}}\cos(\mathbf{Q}_2\cdot\mathbf{R}_l + \varphi_{\mathbf{Q}_2})]\left\{1+\frac{f[\Delta S^{(1)}]}{S}\right\},$$

$$\langle S_l^y\rangle = \pm\sqrt{2S}[\sqrt{\rho_{\mathbf{Q}_1}}\cosh\theta_{\mathbf{Q}_1}^{(1)}\sin\varphi_{\mathbf{Q}_1} + \sqrt{\rho_{\mathbf{Q}_2}}\sin(\mathbf{Q}_2\cdot\mathbf{R}_l + \varphi_{\mathbf{Q}_2})]\left\{1+\frac{f[\Delta S^{(1)}]}{S}\right\}, \quad \text{for } l\in\mathrm{A}$$

$$\langle S_l^z\rangle = [S-\Delta S^{(1)}] - [\rho_{\mathbf{Q}_1}\cosh^2\theta_{\mathbf{Q}_1}^{(1)} + \rho_{\mathbf{Q}_2} + \cosh\theta_{\mathbf{Q}_1}^{(1)}\sqrt{\rho_{\mathbf{Q}_1}\rho_{\mathbf{Q}_2}}\cos(\mathbf{Q}_2\cdot\mathbf{R}_l + \varphi_{\mathbf{Q}_2} - \varphi_{\mathbf{Q}_1})], \tag{A4a}$$

$$\langle S_m^x\rangle = -\sqrt{2S\rho_{\mathbf{Q}_1}}\sinh\theta_{\mathbf{Q}_1}^{(1)}\cos\varphi_{\mathbf{Q}_1}\left(1+\frac{f(\Delta S^{(1)})}{S}\right),$$

$$\langle S_m^y\rangle = \mp\sqrt{2S\rho_{\mathbf{Q}_1}}\sinh\theta_{\mathbf{Q}_1}^{(1)}\sin\varphi_{\mathbf{Q}_1}\left(1+\frac{f(\Delta S^{(1)})}{S}\right),$$

$$\langle S_m^z\rangle = -(S-\Delta S^{(1)}) + \rho_{\mathbf{Q}_1}\sinh^2\theta_{\mathbf{Q}_1}^{(1)}, \quad \text{for } m\in\mathrm{B}, \tag{A4b}$$

where we use $\sinh\theta_{\mathbf{Q}_2}^{(1)}=0$ and ΔS and $f(\Delta S)$ is the same as in Eq. (20a) and (20b). By some numerical calculations, we found that this nontrivial SS phase with $(\varphi_{\mathbf{Q}_1}-\varphi_{\mathbf{Q}_2})=0$ (SS3) is stabilized for a broad region of the parameter space, mainly for $J_2^z>0$. For example, if $J_1^z/|J_1^\perp|=3$ (and $\Lambda=0$), the SS3 exists for $0.2\lesssim J_2^z/|J_1^\perp|\lesssim 2.0$.

For $\Lambda\approx 0$, Γ_2 and Γ_3 may have a influence on the magnetization process around the half-filled solid. For example, if $\Lambda>0$, the system energy is given by

$$\frac{E_{\mathrm{eff}}}{N} \approx \frac{1}{2}\Gamma_{\mathbf{Q}_1}\rho_{\mathbf{Q}_1}^2 + \frac{1}{2}\Gamma_{\mathbf{Q}_2}\rho_{\mathbf{Q}_2}^2 + \Gamma_2\rho_{\mathbf{Q}_1}\rho_{\mathbf{Q}_2} + \Gamma_3\rho_{\mathbf{Q}_1}\rho_{\mathbf{Q}_2}\cos 2(\varphi_{\mathbf{Q}_1}-\varphi_{\mathbf{Q}_2}) - S\mu_0\rho_{\mathbf{Q}_1} + (-S\mu_0+\Delta_2)\rho_{\mathbf{Q}_2}, \tag{A5}$$

where $\Delta_2=\epsilon_{\mathrm{cl}}(\mathbf{Q}_2)-\epsilon_{\mathrm{cl}}(\mathbf{Q}_1)\sim O(\Lambda)>0$ and Γs obtained at $\Lambda=0$ may be used approximately. If the used parameters satisfy the condition of the stability of the SS3 discussed above, a phase transition from SS1 to SS3 occurs at

$$S\mu_{0c1} = \frac{\Gamma_{\mathbf{Q}_1}\Delta_2}{\Gamma_{\mathbf{Q}_1} - (\Gamma_2 - |\Gamma_3|)}. \tag{A6}$$

Then, the densities of the condensed bosons are given by

$$\rho_{\mathbf{Q}_1} = \frac{(\Gamma_{\mathbf{Q}_2} - (\Gamma_2 - |\Gamma_3|))S\mu_0 + (\Gamma_2 - |\Gamma_3|)\Delta_2}{\Gamma_{\mathbf{Q}_1}\Gamma_{\mathbf{Q}_2} - (\Gamma_2 - |\Gamma_3|)^2}, \tag{A7a}$$

$$\rho_{\mathbf{Q}_2} = \frac{(\Gamma_{\mathbf{Q}_1} - (\Gamma_2 - |\Gamma_3|))S\mu_0 - \Gamma_{\mathbf{Q}_1}\Delta_2}{\Gamma_{\mathbf{Q}_1}\Gamma_{\mathbf{Q}_2} - (\Gamma_2 - |\Gamma_3|)^2}. \tag{A7b}$$

At $\mu_0 = \mu_{0c1}$, Eqs. (A7) and (22) give the same density $\rho_{\mathbf{Q}_{1,2}}$, and thus a second-order phase transition is implied. If $\Lambda < 0$, similarly, a second-order phase transition from SS2 to SS3 occurs at

$$S\mu_{0c2} = \frac{\Gamma_{\mathbf{Q}_2}\Delta_1}{\Gamma_{\mathbf{Q}_2} - (\Gamma_2 - |\Gamma_3|)}. \tag{A8}$$

where $\Delta_1 = -\Delta_2$.

APPENDIX B: SOME EQUATIONS OMITTED IN THE TEXT

1. Section IV B

The additional quadratic terms in Eq. (39) emerging from normal order of the Bogoliubov-transformed bosons are given by

$$T_1(\mathbf{k}) = \epsilon_0(\mathbf{k})\left(\frac{1}{N}\sum_{\mathbf{q}} \sinh^2\theta_q\right) - J_1^{\perp}\left(\frac{1}{N}\sum_{\mathbf{q}} C_1(\mathbf{q})\sinh 2\theta_q\right) + \left(-\frac{2}{3}J_2^z C_2(\mathbf{k}) + 2J_2^{\perp}\right)\left(\frac{1}{N}\sum_{\mathbf{q}} C_2(\mathbf{q})\sinh^2\theta_q\right),$$

$$T_2(\mathbf{k}) = t_0(\mathbf{k})\left(\frac{1}{N}\sum_{\mathbf{q}} \sinh^2\theta_q\right) - \frac{J_1^z}{4}C_1(k) \times\left(\frac{1}{N}\sum_{\mathbf{q}} C_1(\mathbf{q})\sinh 2\theta_q\right), \tag{B1}$$

2. Section V B

The interaction part of Hamiltonian which contributes to the kernel of the order of $(J_1^z)^{-1}$ is given by

$$\begin{aligned} H_{(\mathrm{I2})\mathrm{int}} = \frac{1}{N}\sum_{\mathbf{q},\mathbf{k}_1,\mathbf{k}_2} \{&(J_2^z C_2(\mathbf{q}) - J_2^{\perp}C_2(\mathbf{k}_2) \\ &- 2J_1^z \sinh\theta_{\mathbf{k}_2-\mathbf{q}} \sinh\theta_{\mathbf{k}_2} C_1(\mathbf{q}) \\ &+ J_1^{\perp}C_1(\mathbf{k}_2)\sinh\theta_{\mathbf{k}_2})\alpha^{\dagger}_{\mathbf{k}_1+\mathbf{q}}\alpha^{\dagger}_{\mathbf{k}_2-\mathbf{q}}\alpha_{\mathbf{k}_1}\alpha_{\mathbf{k}_2} \\ &- 2J_1^z C_1(\mathbf{q})\alpha^{\dagger}_{\mathbf{k}_1+\mathbf{q}}\beta^{\dagger}_{\mathbf{k}_2-\mathbf{q}}\alpha_{\mathbf{k}_1}\beta_{\mathbf{k}_2} \\ &+ 2J_1^z C_1(\mathbf{q})\sinh\theta_{\mathbf{k}_2+\mathbf{q}}\alpha^{\dagger}_{\mathbf{k}_1+\mathbf{q}}\alpha_{\mathbf{k}_2+\mathbf{q}}\alpha_{\mathbf{k}_1}\beta_{-\mathbf{k}_2} \\ &+ (2J_1^z C_1(\mathbf{q})\sinh\theta_{\mathbf{k}_2-\mathbf{q}} \\ &- J_1^{\perp}C_1(\mathbf{k}_2))\alpha^{\dagger}_{\mathbf{k}_1+\mathbf{q}}\alpha^{\dagger}_{\mathbf{k}_2-\mathbf{q}}\alpha_{\mathbf{k}_1}\beta^{\dagger}_{-\mathbf{k}_2}\} \end{aligned} \tag{B2}$$

[1] O. Penrose and L. Onsager, Phys. Rev. **104**, 576 (1956).
[2] A. Andreev and I. Lifshits, Sov. Phys. JETP **29**, 1107 (1969).
[3] G. V. Chester, Phys. Rev. A **2**, 256 (1970).
[4] E. Kim and M. H. W. Chan, Nature (London) **427**, 225 (2004); Science **305**, 1941 (2004).
[5] A. J. Leggett, Phys. Rev. Lett. **25**, 1543 (1970).
[6] M. Boninsegni, N. Prokof'ev, and B. Svistunov, Phys. Rev. Lett. **96**, 105301 (2006); G. Biroli, C. Chamon, and F. Zamponi, Phys. Rev. B **78**, 224306 (2008); P. W. Anderson, Science **324**, 631 (2009); For reviews, see, D. E. Galli and L. Reatto, J. Phys. Soc. Jpn. **77**, 111010 (2008).
[7] T. Matsubara and H. Matsuda, Prog. Theor. Phys. **16**, 569 (1956); **17**, 19 (1957).
[8] H. Matsuda and T. Tsuneto, Prog. Theor. Phys. **46**, 411 (1970).
[9] K.-S. Liu and M. E. Fisher, J. Low Temp. Phys. **10**, 655 (1973).
[10] G. G. Batrouni and R. T. Scalettar, Phys. Rev. Lett. **84**, 1599 (2000).
[11] F. Hebert, G. G. Batrouni, R. T. Scalettar, G. Schmid, M. Troyer, and A. Dorneich, Phys. Rev. B **65**, 014513 (2001).
[12] Y. C. Chen, R. G. Melko, S. Wessel, and Y. J. Kao, Phys. Rev. B **77**, 014524 (2008); L. Dang, M. Boninsegni, and L. Pollet, *ibid.* **78**, 132512 (2008); K. K. Ng, Y. C. Chen, and Y. C. Tzeng, arXiv:0908.2478 (unpublished).
[13] T. Nikuni, M. Oshikawa, A. Oosawa, and H. Tanaka, Phys. Rev. Lett. **84**, 5868 (2000).
[14] T. Radu, H. Wilhelm, V. Yushankhai, D. Kovrizhin, R. Coldea, Z. Tylczynski, T. Lühmann, and F. Steglich, Phys. Rev. Lett. **95**, 127202 (2005).
[15] T. Giamarchi, C. Rüegg, and O. Tchernyshyov, Nat. Phys. **4**, 198 (2008).
[16] M. Takigawa, S. Matsubara, M. Horvatic, C. Berthier, H. Kageyama, and Y. Ueda, Phys. Rev. Lett. **101**, 037202 (2008).
[17] H. Kageyama, K. Yoshimura, R. Stern, N. V. Mushnikov, K. Onizuka, M. Kato, K. Kosuge, C. P. Slichter, T. Goto, and Y. Ueda, Phys. Rev. Lett. **82**, 3168 (1999).
[18] T. Momoi and K. Totsuka, Phys. Rev. B **62**, 15067 (2000).
[19] K. Penc, J.-B. Fouet, S. Miyahara, O. Tchernyshyov, and F. Mila, Phys. Rev. Lett. **99**, 117201 (2007).
[20] S. T. Beliaev, Sov. Phys. JETP **7**, 299 (1958).
[21] E. G. Batyev and L. S. Braginskii, Zh. Eksp. Teor. Fiz. **87**, 1361 (1984) [Sov. Phys. JETP **60**, 781 (1984)]; E. G. Batyev, Zh. Eksp. Teor. Fiz. **89**, 308 (1985) [Sov. Phys. JETP **62**, 173 (1985)].
[22] T. Nikuni and H. Shiba, J. Phys. Soc. Jpn. **64**, 3471 (1995).
[23] A. V. Chubukov, Phys. Rev. B **44**, 4693 (1991).
[24] H. T. Ueda and K. Totsuka, Phys. Rev. B **80**, 014417 (2009); H. T. Ueda, K. Totsuka, and T. Momoi, arXiv:0911.2186, J. Phys.: Conf. Ser. (to be published).
[25] M. Y. Veillette and J. T. Chalker, Phys. Rev. B **74**, 052402 (2006).

[26] T. Suzuki and N. Kawashima, Phys. Rev. B **75**, 180502(R) (2007).
[27] F. Mila, J. Dorier, and K. P. Schmidt, Prog. Theor. Phys. **176**, 355 (2008).
[28] K.-K. Ng and T. K. Lee, Phys. Rev. Lett. **97**, 127204 (2006); K. P. Schmidt, J. Dorier, A. M. Läuchli, and F. Mila, *ibid.* **100**, 090401 (2008).
[29] G. G. Batrouni, R. T. Scalettar, G. T. Zimanyi, and A. P. Kampf, Phys. Rev. Lett. **74**, 2527 (1995).
[30] R. T. Scalettar, G. G. Batrouni, A. P. Kampf, and G. T. Zimanyi, Phys. Rev. B **51**, 8467 (1995).
[31] C. Pich and E. Frey, Phys. Rev. B **57**, 13712 (1998).
[32] J. Oitmaa and W. Zheng, Phys. Rev. B **69**, 064416 (2004); K. Majumdar and T. Datta, J. Phys.: Condens. Matter **21**, 406004 (2009) and references cited therein.
[33] M. P. A. Fisher, P. B. Weichman, G. Grinstein, and D. S. Fisher, Phys. Rev. B **40**, 546 (1989).
[34] F. J. Dyson, Phys. Rev. **102**, 1217 (1956); S. V. Maleev, J. Exp. Theor. Phys. **33**, 1010 (1957) Sov. Phys. JETP **6**, 776 (1958).
[35] T. Oguchi, Prog. Theor. Phys. **25**, 721 (1961); T. Oguchi and A. Honma, J. Appl. Phys. **34**, 1153 (1963).
[36] M. Takahashi, Phys. Rev. B **40**, 2494 (1989).
[37] H. Shi and A. Griffin, Phys. Rep. **304**, 1 (1998).
[38] A. J. Stoffel and M. Gulácsi, Eur. Phys. Lett. **85**, 20009 (2009); Eur. Phys. J. B **67**, 169 (2009); **68**, 79 (2009); Philos. Mag. **89**, 2043 (2009).
[39] In Sec. III modelgeneral; the hermiticity of the Hamiltonian is assumed. In general, the nonhermitian DM Hamiltonian H_{DM} is given by $U^{-1}H_{\mathrm{HP}}U$, where H_{HP} is the Holstein-Primakoff transformed Hamiltonian and U is the nonunitary operator, which recovers the hermiticity of H_{DM}.[35] In NAF phase, we may not consider the effect of U when we calculates the observables since the ground state (vacuum) is the eigenstate of U. If the boson condenses, U may shift the vacuum and we must manipulate the operator U explicitly. However, since we consider only a dilute-gas limit and need the observables obtained in the NAF phase (at $\mu_\alpha=0^-$), the hermiticity does not matter in the concrete discussion.
[40] When there exist degenerate minima at several **Q**s, there is a possibility that the bosons at different **Q**s simultaneously condense and the magnetic structure may be different from the one characterized by Eq. (20a) and (20b). See Appendix A for more detail.
[41] The analysis near the saturation field is free from this problem; the fully polarized state is an exact eigenstate and high enough magnetic field guarantees the validity of the reference state.